DTU Library

European wind resource mapping by satellite images

Hasager, Charlotte Bay; Badger, Merete; Pena Diaz, Alfredo; Hahmann, Andrea N.; Badger, Jake; Karagali, Ioanna

Publication date:
2015

Document Version
Peer reviewed version

[Link back to DTU Orbit](#)

Citation (APA):
Hasager, C. B. (Author), Badger, M. (Author), Pena Diaz, A. (Author), Hahmann, A. N. (Author), Badger, J. (Author), & Karagali, I. (Author). (2015). European wind resource mapping by satellite images. Sound/Visual production (digital)

European wind resource mapping by satellite images

Charlotte Hasager, Merete Badger, Alfredo Peña, Andrea Hahmann, Jake Badger, Ioanna Karagali

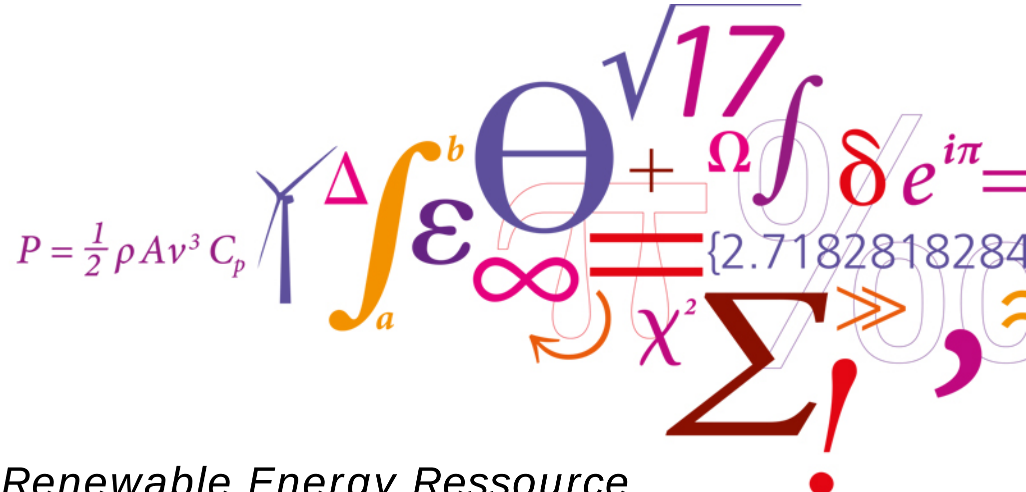

ISES Solar World Congress, Forum Renewable Energy Ressource Assessment and Mapping, Daegu, South Korea, 8-12 November 2015

DTU Wind Energy
Department of Wind Energy

Content

- Motivation for offshore wind ressource mapping from satellites
- Synthetic Aperture Radar surface ocean wind fields
- DTU Wind Energy processing chain
- Applications
    - Wind ressource mapping
    - Model verification
    - Wind farm wakes
- Lifting winds to hub-height
- Summary on advantages and limitations of SAR in wind energy
- Acknowledgements

Offshore wind energy perspectives

- By the end of July 2015 a European total of 3,072 offshore turbines are installed and connected to the grid, totaling a cumulative production capacity of *10 GW.*

- The European Wind Energy Association has identified 26 GW of consented offshore wind farms in Europe and future plans for offshore wind farms totaling more than 98 GW.

- China (10 GW plan)
- Japan (1.45 GW plan investigation)
- South Korea (4.5 GW plans)
- Taiwan (600 MW by 2020)
- USA (according to the US Department of Energy 22 GW can come from offshore by 2030)

Sources: www.ewea.org and www.gwec.net

North Sea offshore wind farms map

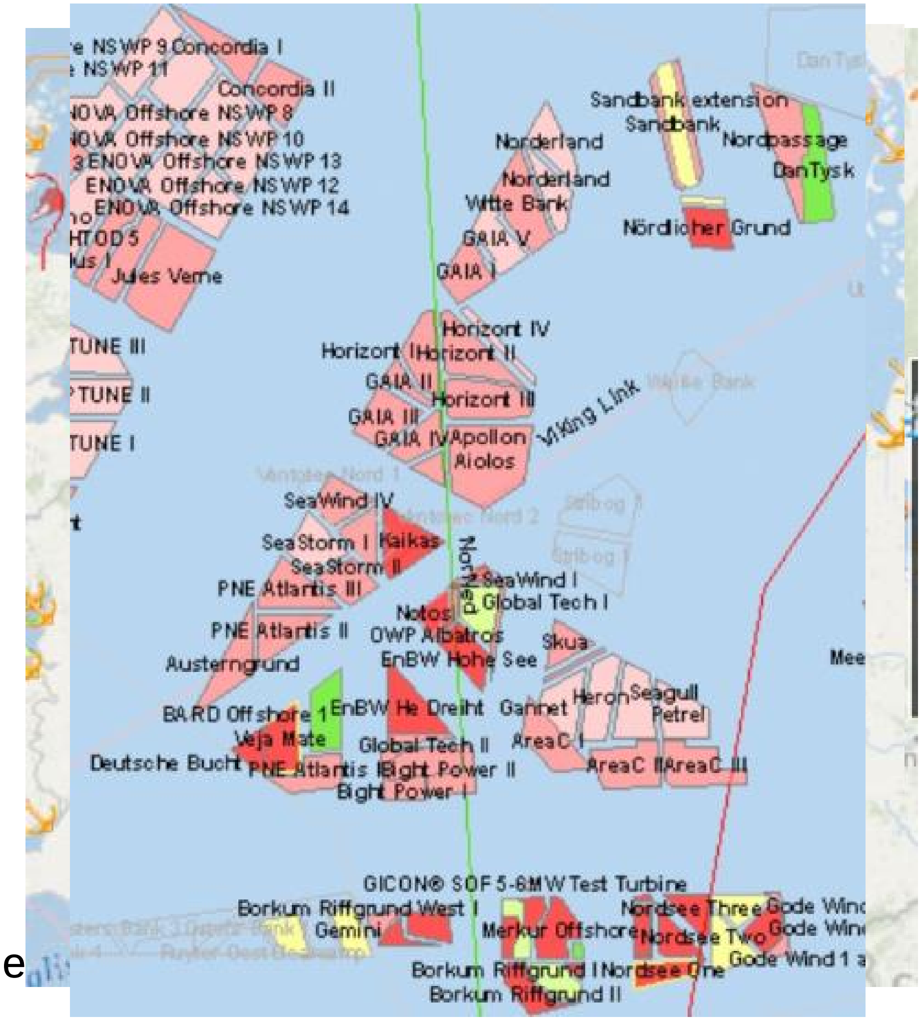

Source: C4Offshore

Motivation for satellite data

- Rapid growth in offshore wind energy

- For a decrease in uncertainty on the predicted mean wind speed at hub height of 0.1 $m \cdot s^{-1}$ there is an estimated saving worth around £10 million per year for 25 years for a large offshore wind farm project according to industry experts[1]

- Installation of met-masts, floating lidar and lidar on platforms costly

- Meteorological modelling possible accurate around 5%

- Satellite data is on the shelf. Desk-top work is fast but it needs experts.

[1]Hasager *et al.* 2013, Hub Height Ocean Winds over the North Sea Observed by the NORSEWInD Lidar Array: Measuring Techniques, Quality Control and Data Management, *Remote Sensing* 2013, *5*(9), 4280-4303; doi:10.3390/rs5094280)

Ocean winds from satellites

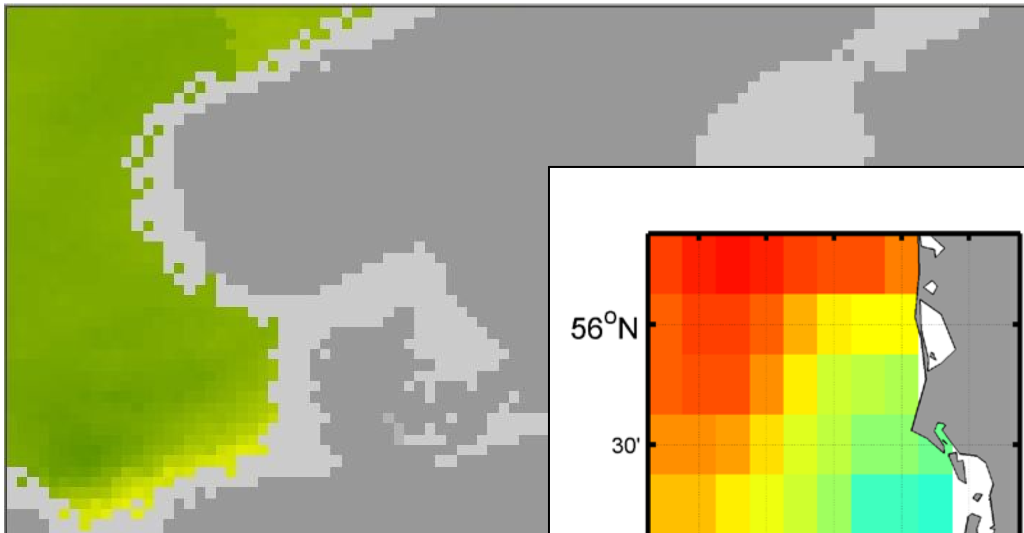

Radiometers (SSM/I)

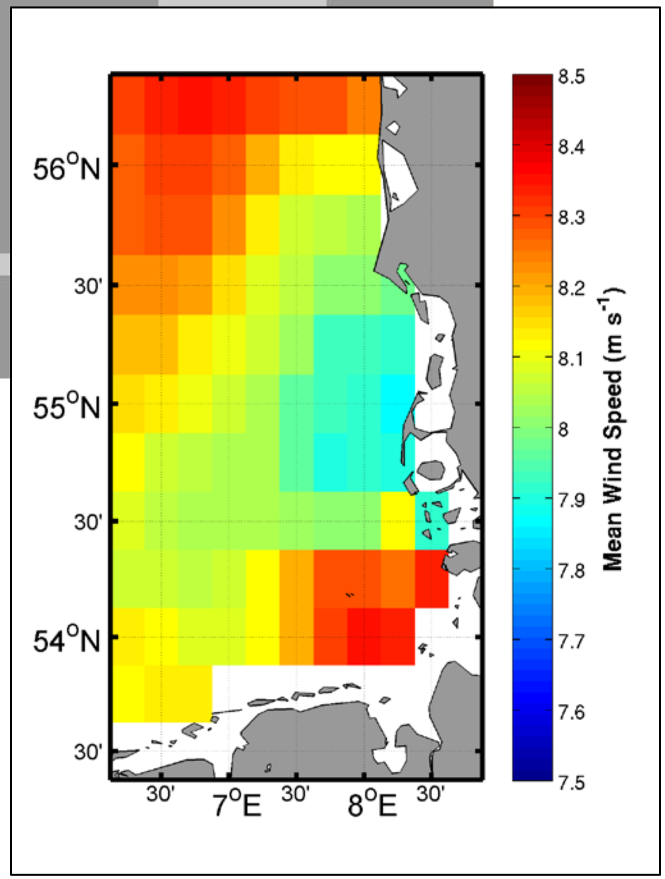

Scatterometers (QuikScat)

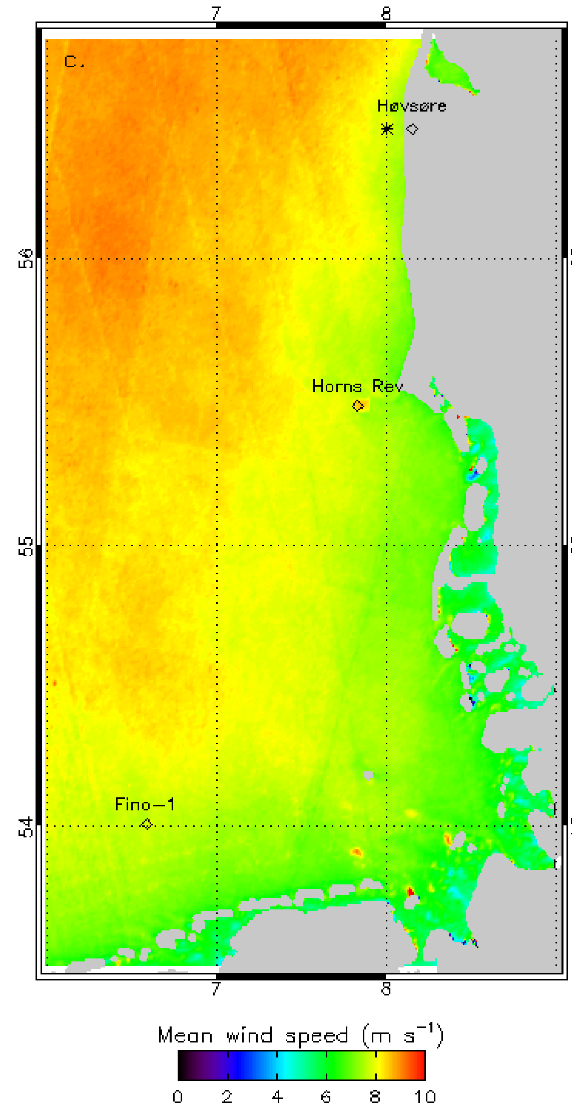

Synthetic Aperture Radar (Envisat ASAR)

Ocean wind fields from satellites

	Radiometer	Scatterometer	Synthetic Aperture Radar (SAR)
Retrieved parameters	Wind speed	Wind speed and direction	Wind speed
Spatial resolution	0.25° lat/lon	0.25° lat/lon	500 m
Spatial coverage	Global	Global	Selected areas
Coastal mask	Cover open oceans only	Up to 70 km from coastline	None
Temporal resolution	4-6 times per day	Twice daily	Variable – less than one per day
Temporal coverage	Systematically since 1987	Systematically since 1991	ScanSAR since 1995
Current sensors	SSM/I (F15, F16, F17)	ASCAT-1/2, HY2A,	Radarsat-1/2, TerraSAR-X, TanDEM-X, COSMO-SkyMed, Sentinel-1
Rain sensitivity	High (rain flags)	Low	Low

The SAR data archive at DTU Wind Energy

~15,000 ENVISAT ASAR scenes from ESA (2002-2011)

~10,000 Sentinel-1 scenes from ESA (2014 ->)

Northern Europe

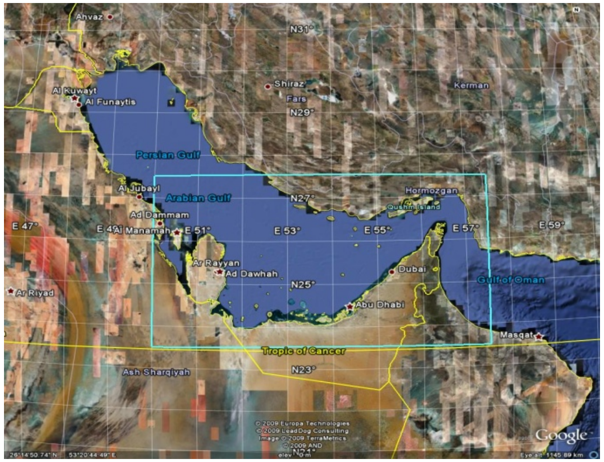

United Arab Emirates

Great Lakes

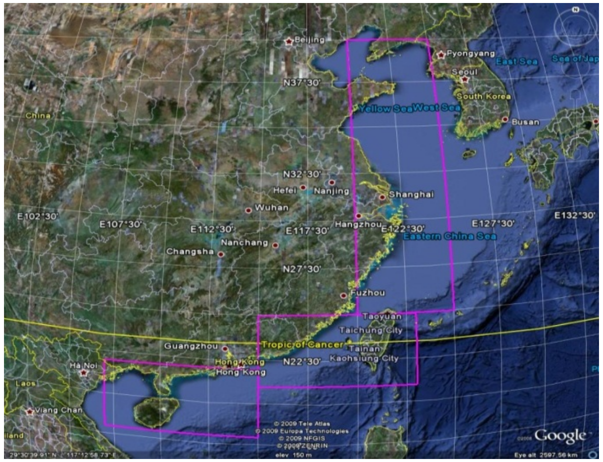

China

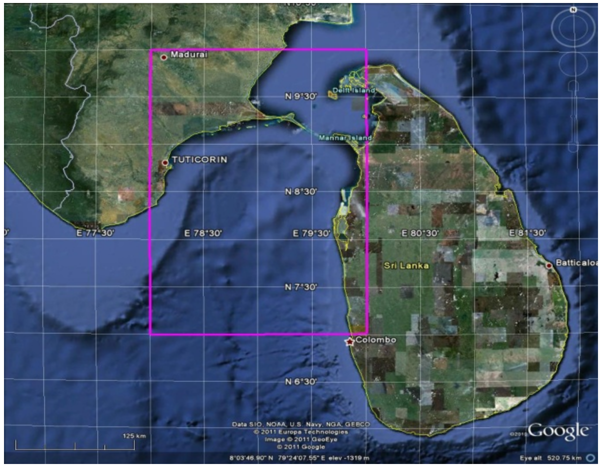

India

The New European Wind Atlas

SAR image coverage

Images frames over a given site have different spatial coverage and orientation

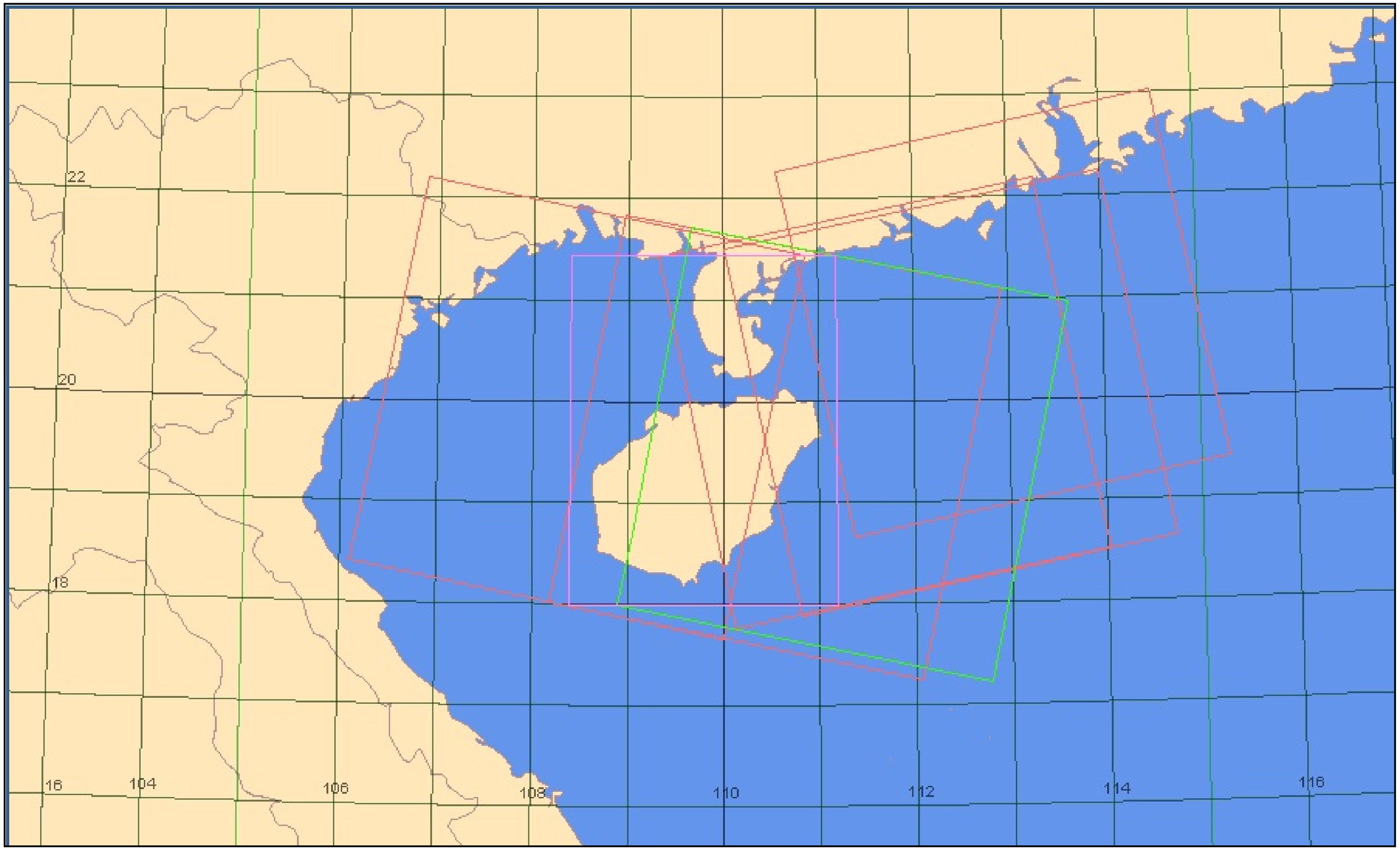

SAR image characteristics

- Image calibration is necessary
- Incidence angle dependency must be accounted for
- Projection to a geographical coordinate system is needed

Original brightness image

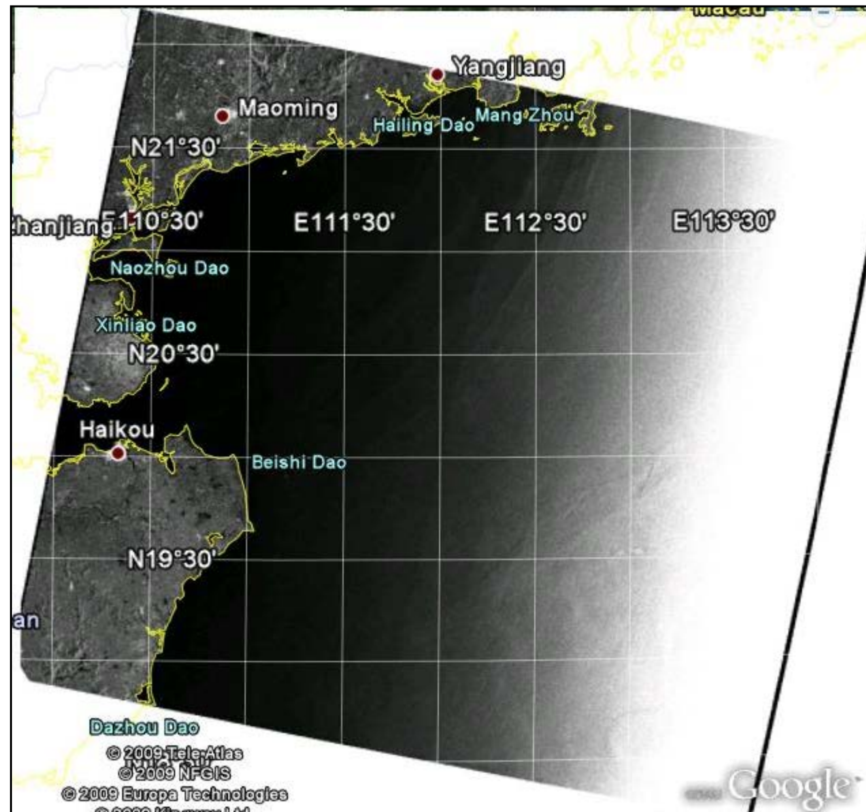

Projected brightness image

SAR wind retrieval

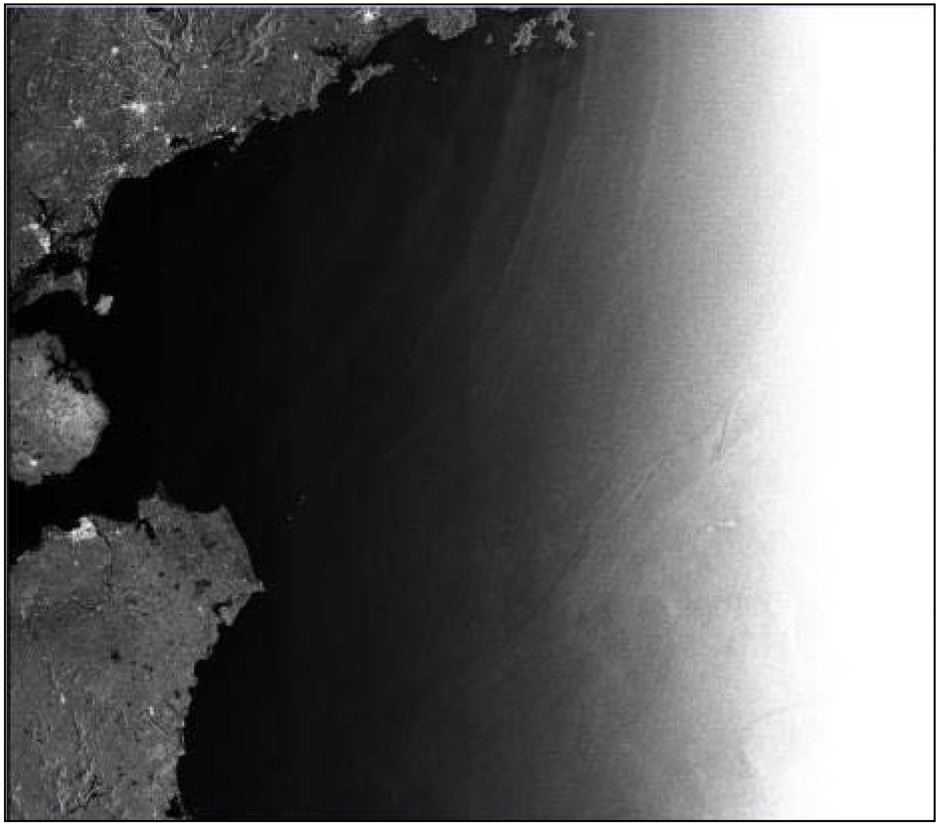

Original brightness image

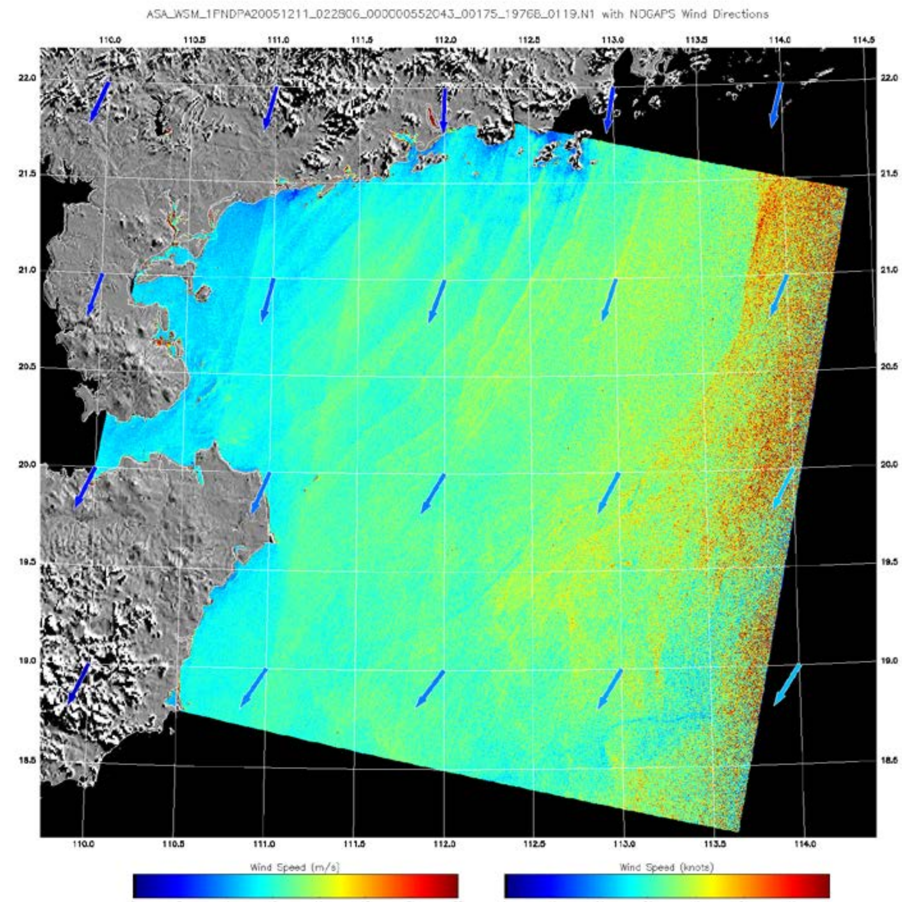

Wind speed map

From wind to radar backscatter

Bragg / resonance scattering:

$$\lambda_{Bragg} = \frac{\lambda_{radar}}{2\sin\theta}$$

θ = incidence angle (15-70°)
λ = wave length (cm scale)

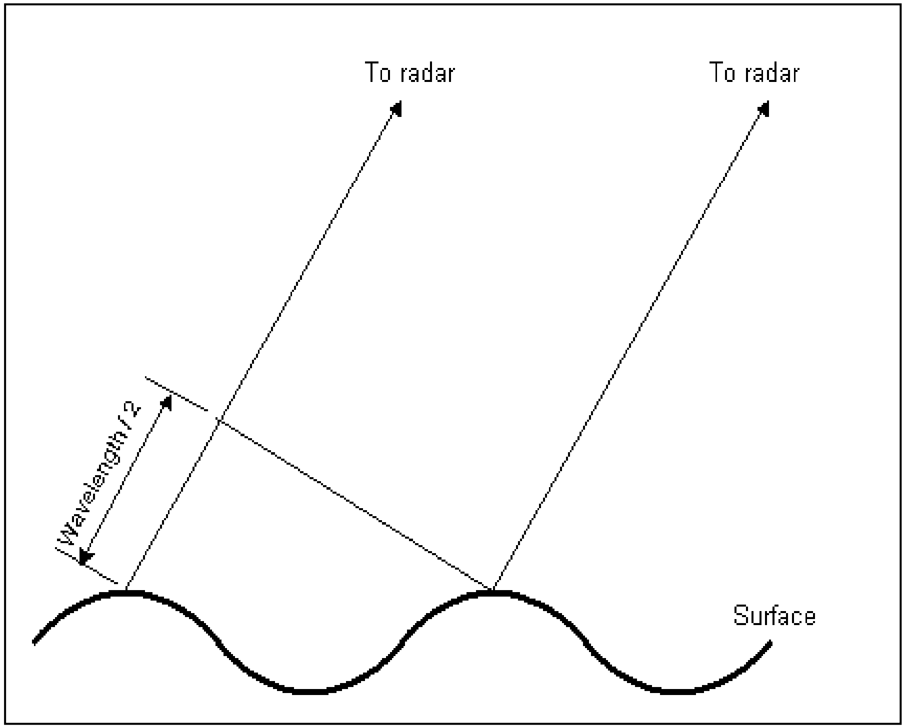

Bragg waves ride on longer-period waves
Random variation occurs (speckle) $\longrightarrow$ Pixel averaging is necessary

From radar backscatter to wind

Empirical geophysical model functions (GMF):

$$NRCS = U^{\gamma(\theta)} A(\theta) \left[1 + B(\theta, U) \cos\phi + C(\theta, U) \cos 2\phi \right]$$

$NRCS$ = radar backscatter [dB]

θ = incidence angle [degrees]

U = wind speed at 10 m [m/s]

Φ = relative wind direction [degrees]

Model functions apply to open oceans and neutral atmospheric stability
The nominal accuracy on wind speed is +/- 2 m/s

Accuracy of the wind direction input

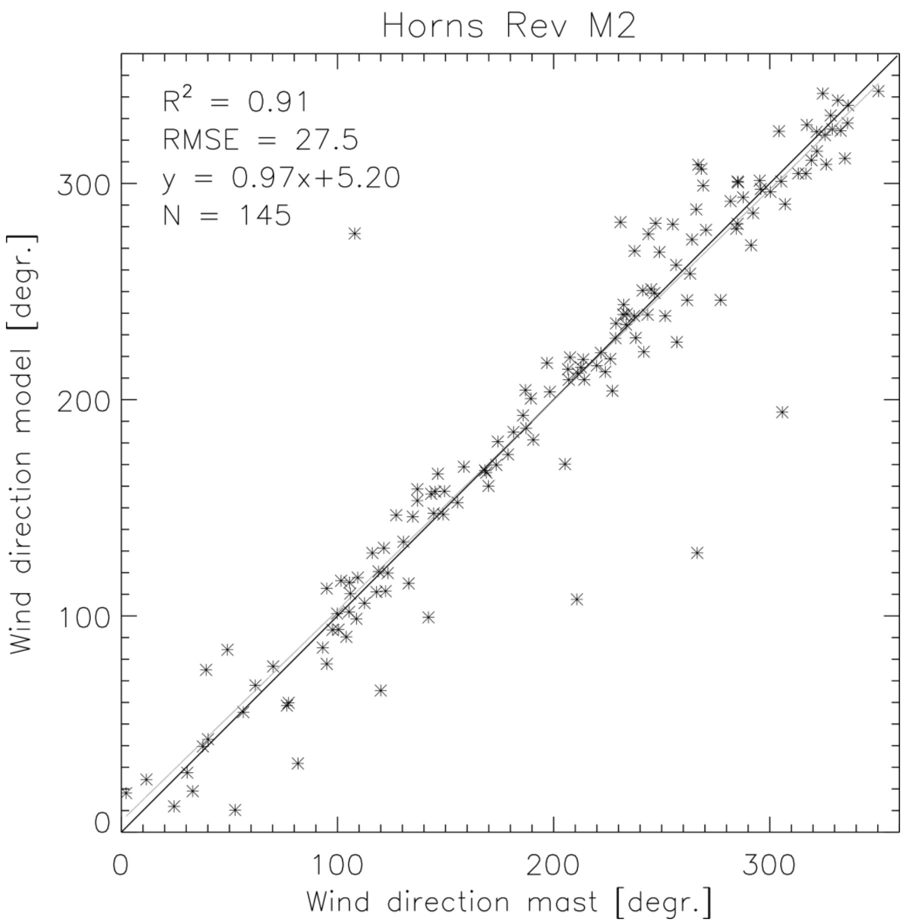

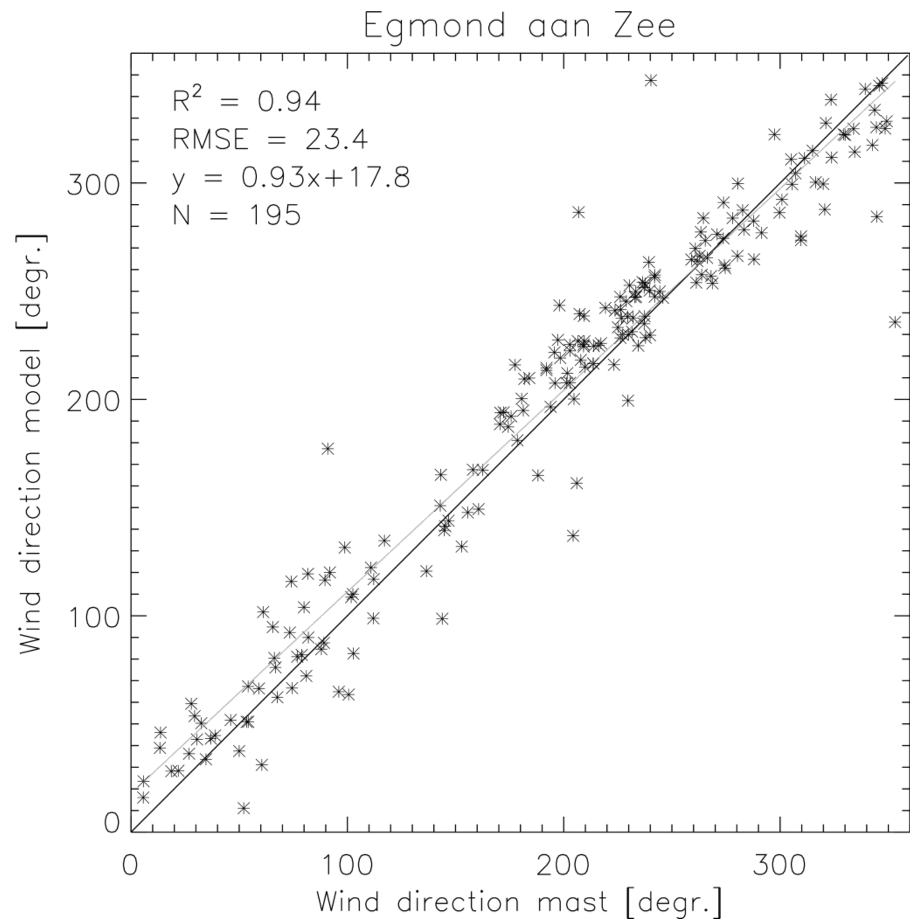

Accuracy of the wind speed retrieval at 10 m

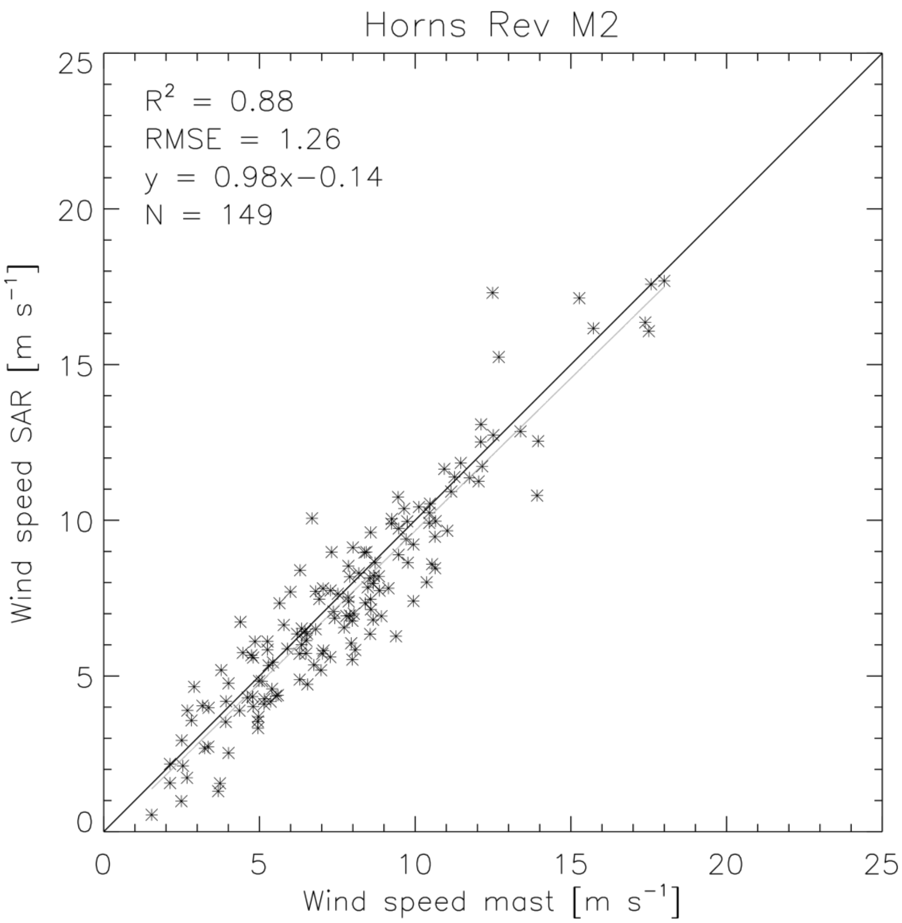

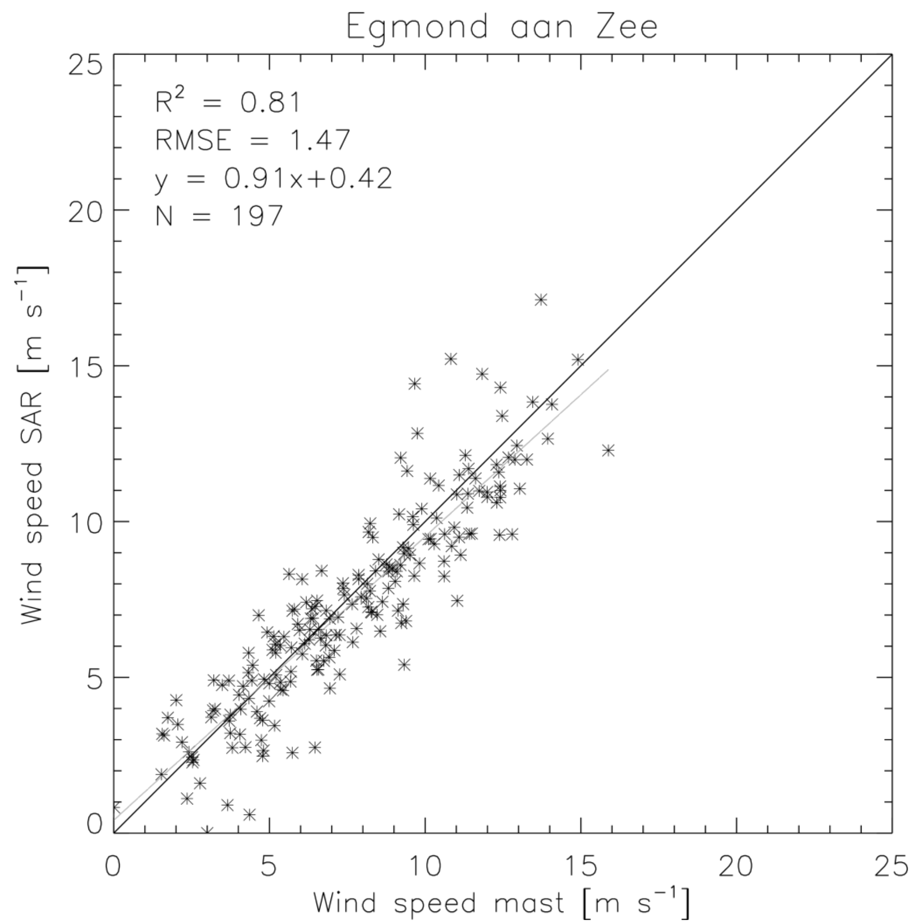

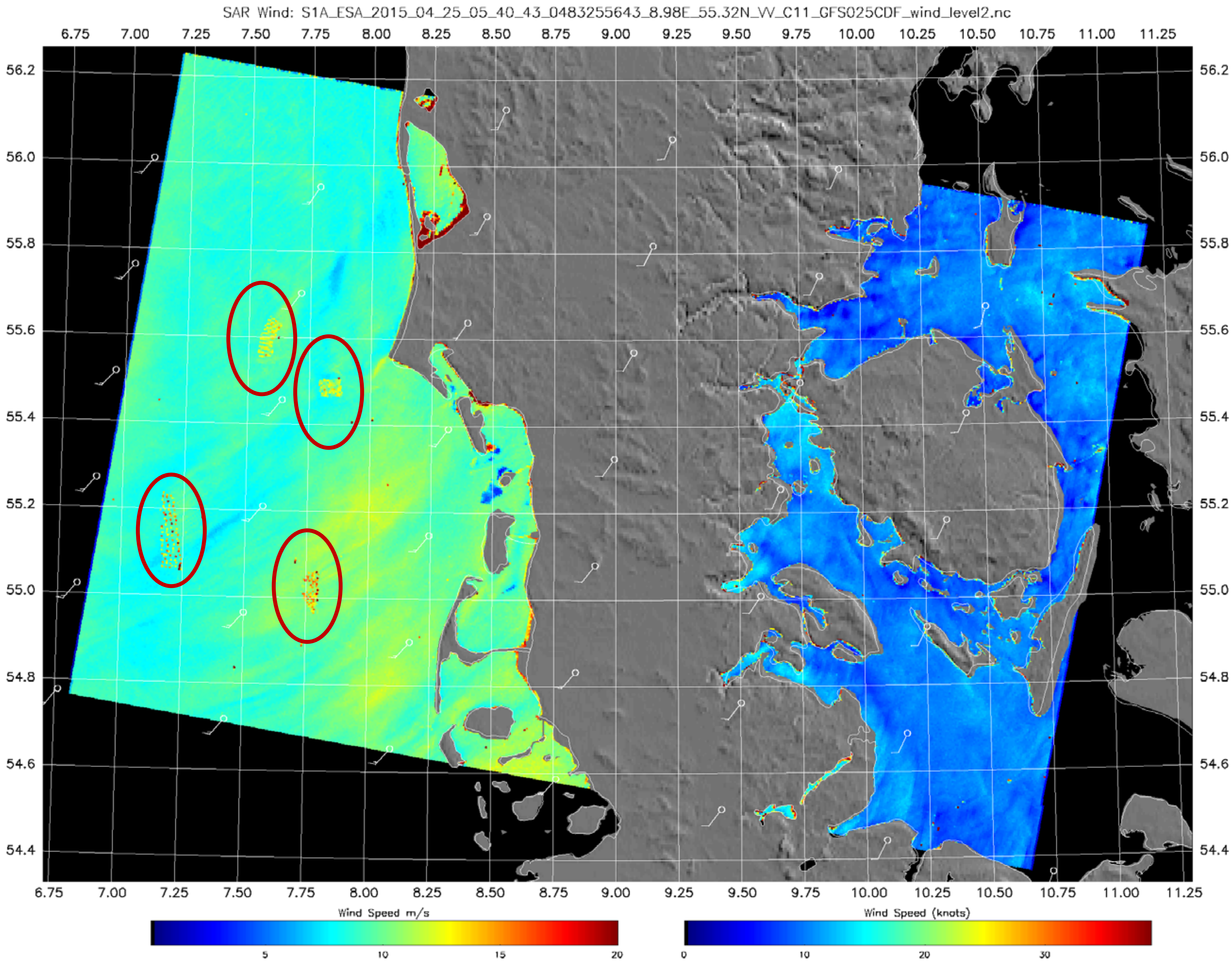

Technical University of Denmark

Processed at DTU Wind Energy 2015 Apr 28 11:56:48 UTC

Wind field retrieved from Sentinel-1a, 25 April 2015 at 05:40 UTC

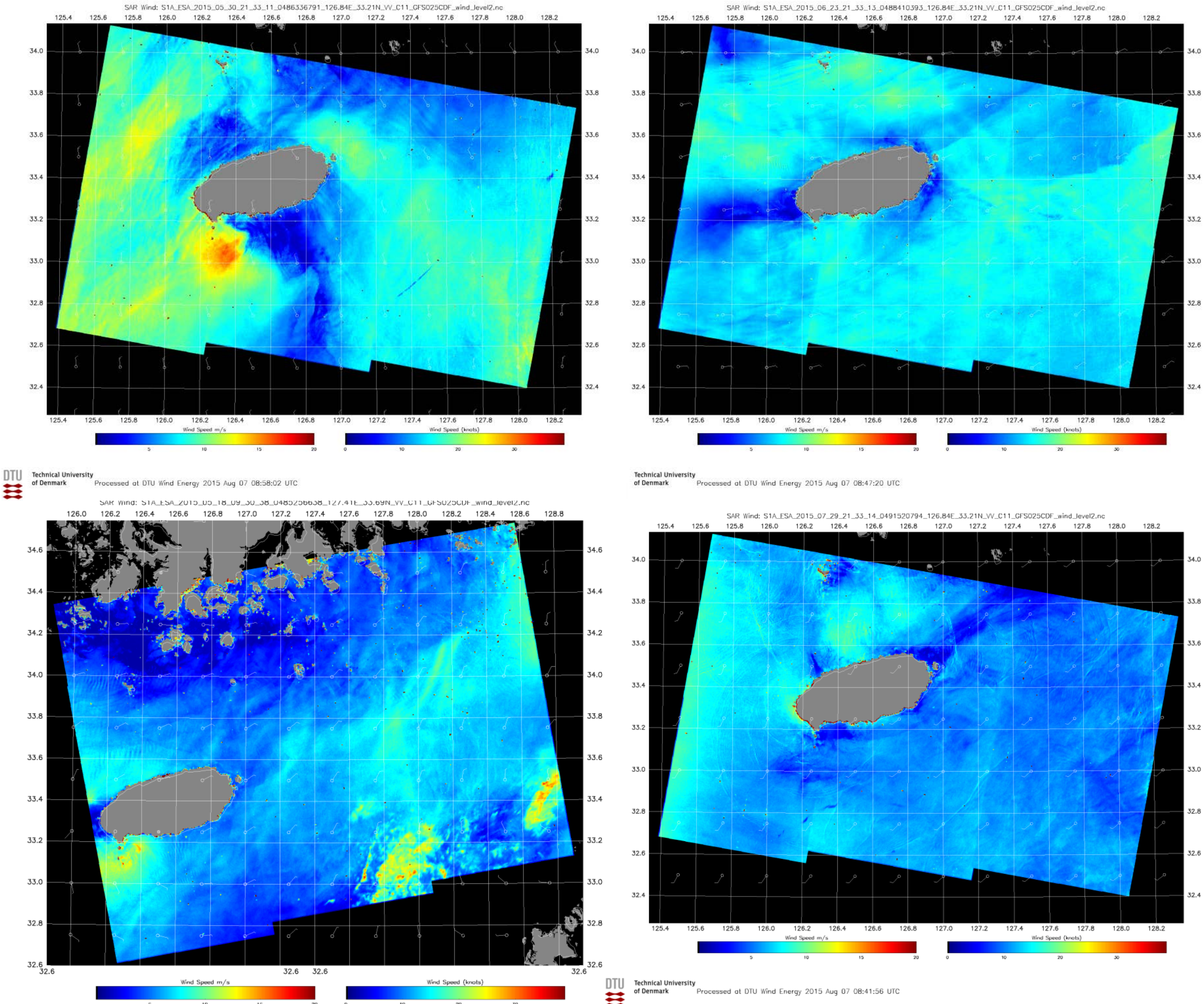

Wind fields retrieved from Sentinel-1a over Jeju Island, South Korea

DTU Wind energy processing chain

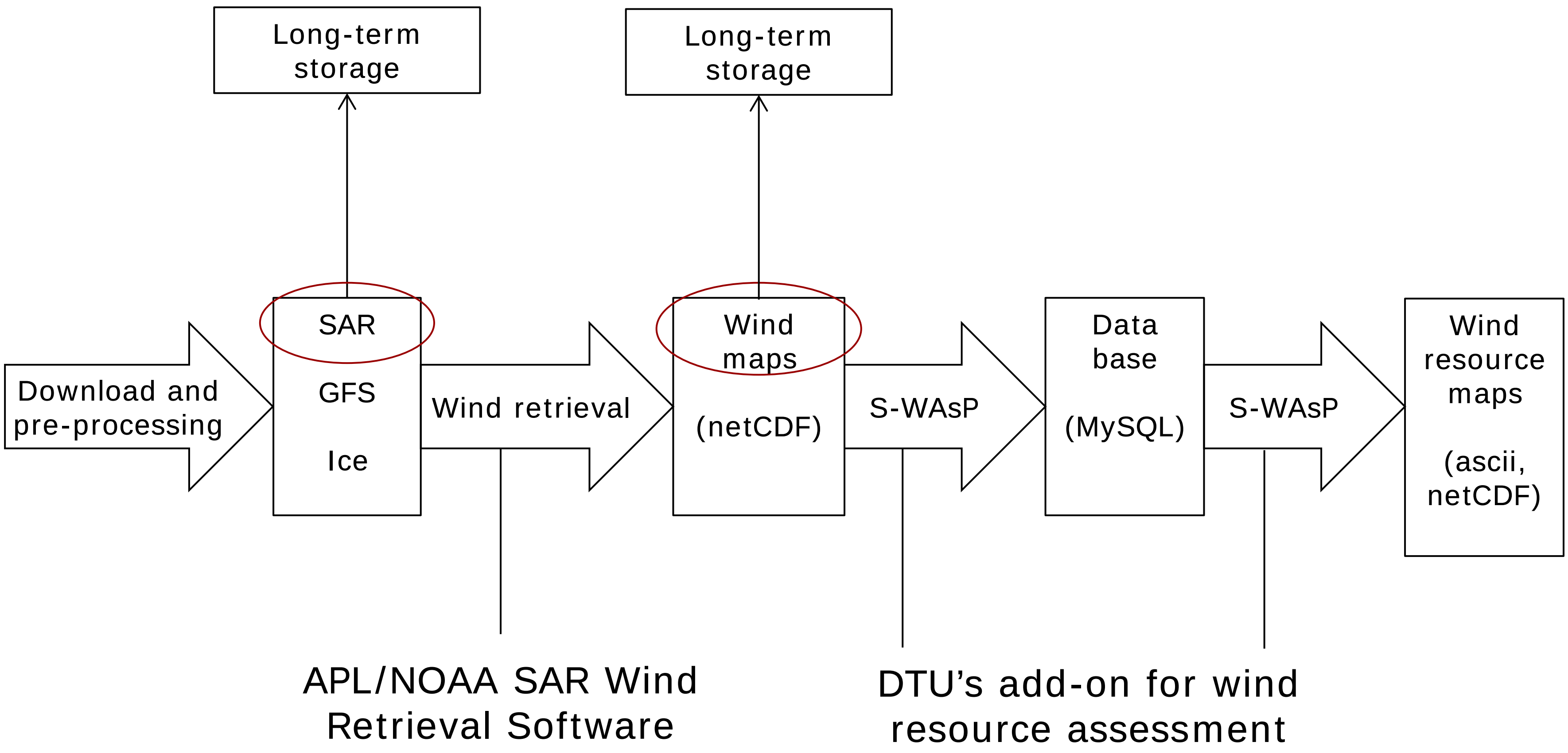

Wind resource mapping

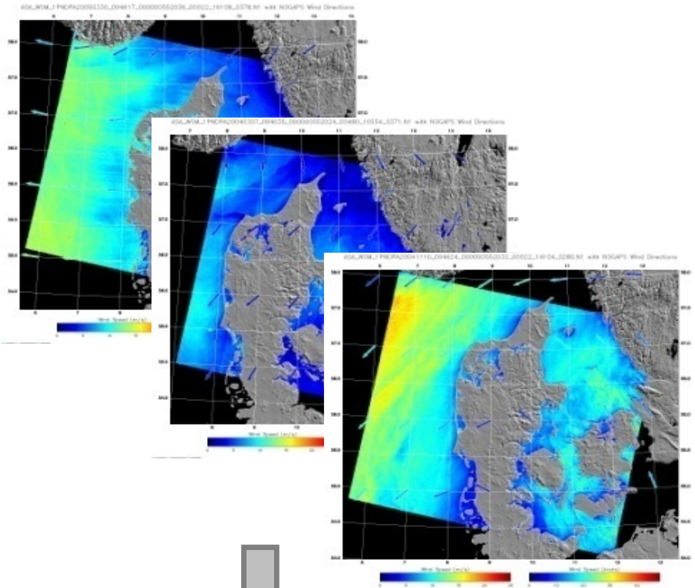

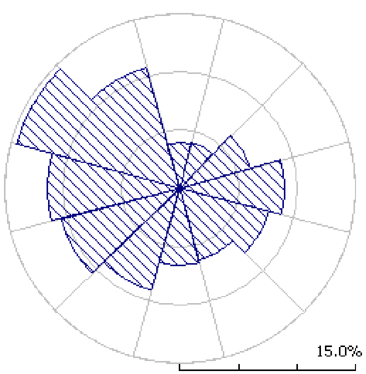

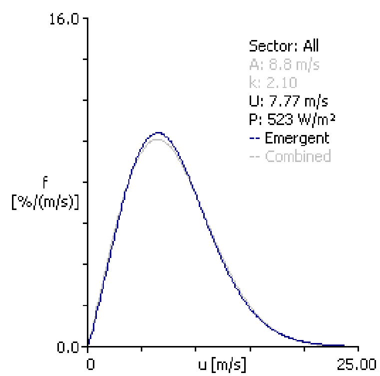

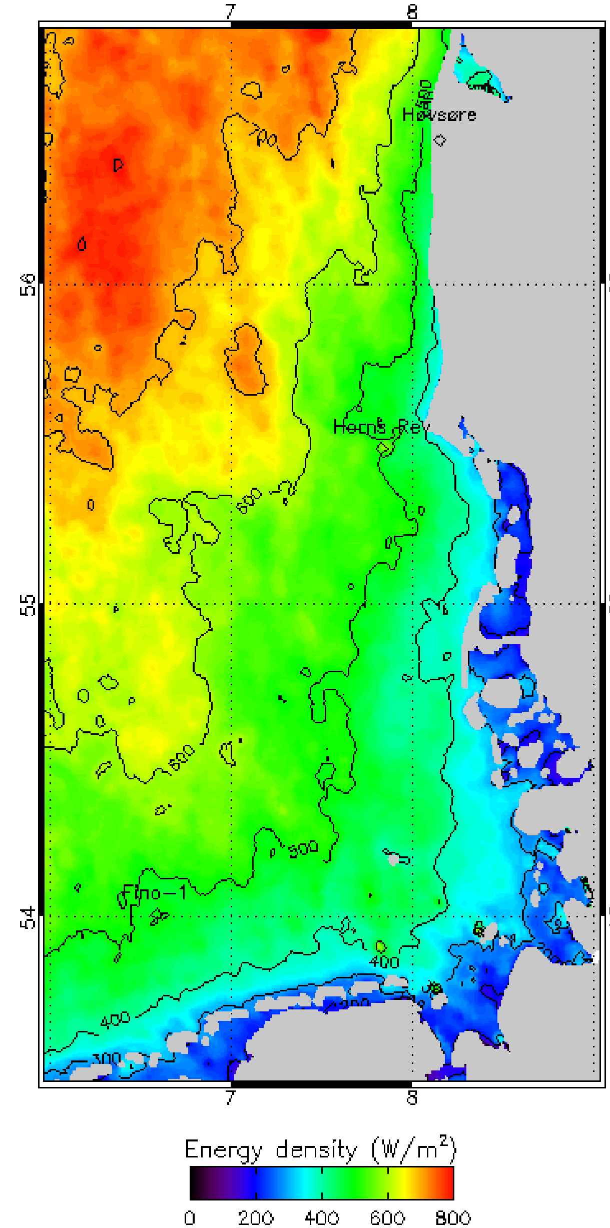

NORSEWInD 10-m wind atlas from SAR

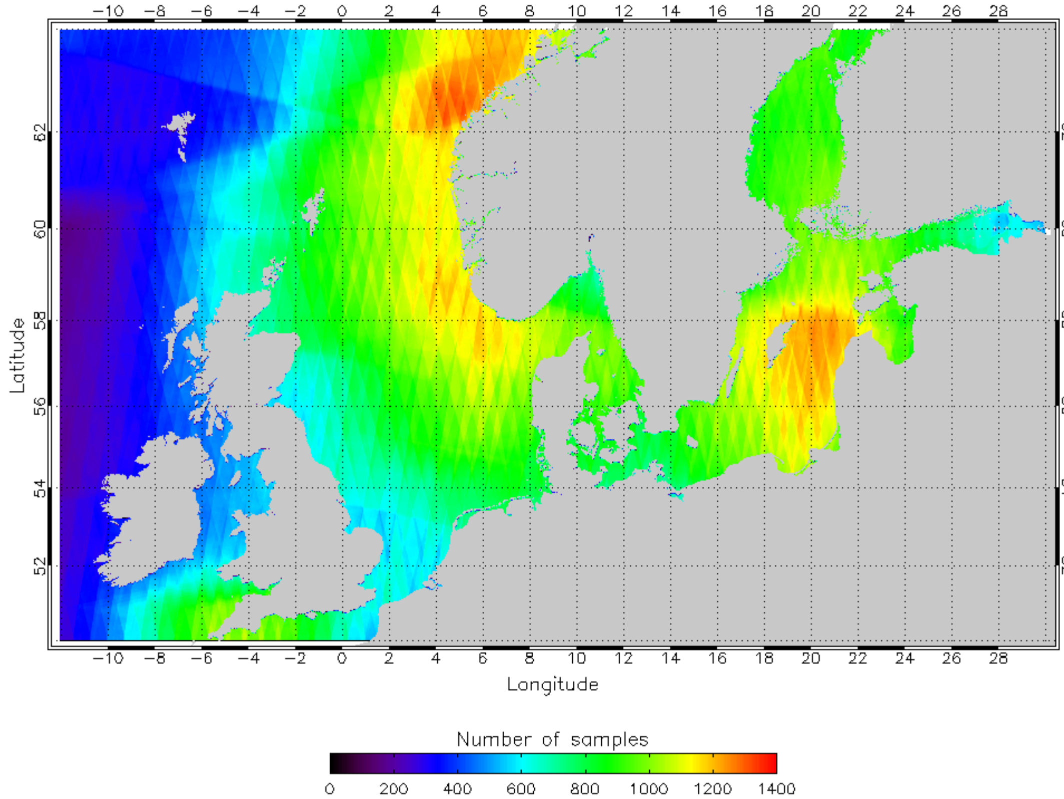

Hasager, C.B., Mouche, A., Badger, M., Bingöl, F., Karagali, I., Driesenaar, T., Stoffelen, A., Peña, A., Longépé, N. (2015) Offshore wind climatology based on synergetic use of Envisat ASAR, ASCAT and QuikSCAT. *Remote Sensing of Environment.*, 156, 247-263, DOI 10.1016/j.rse.2014.09.030

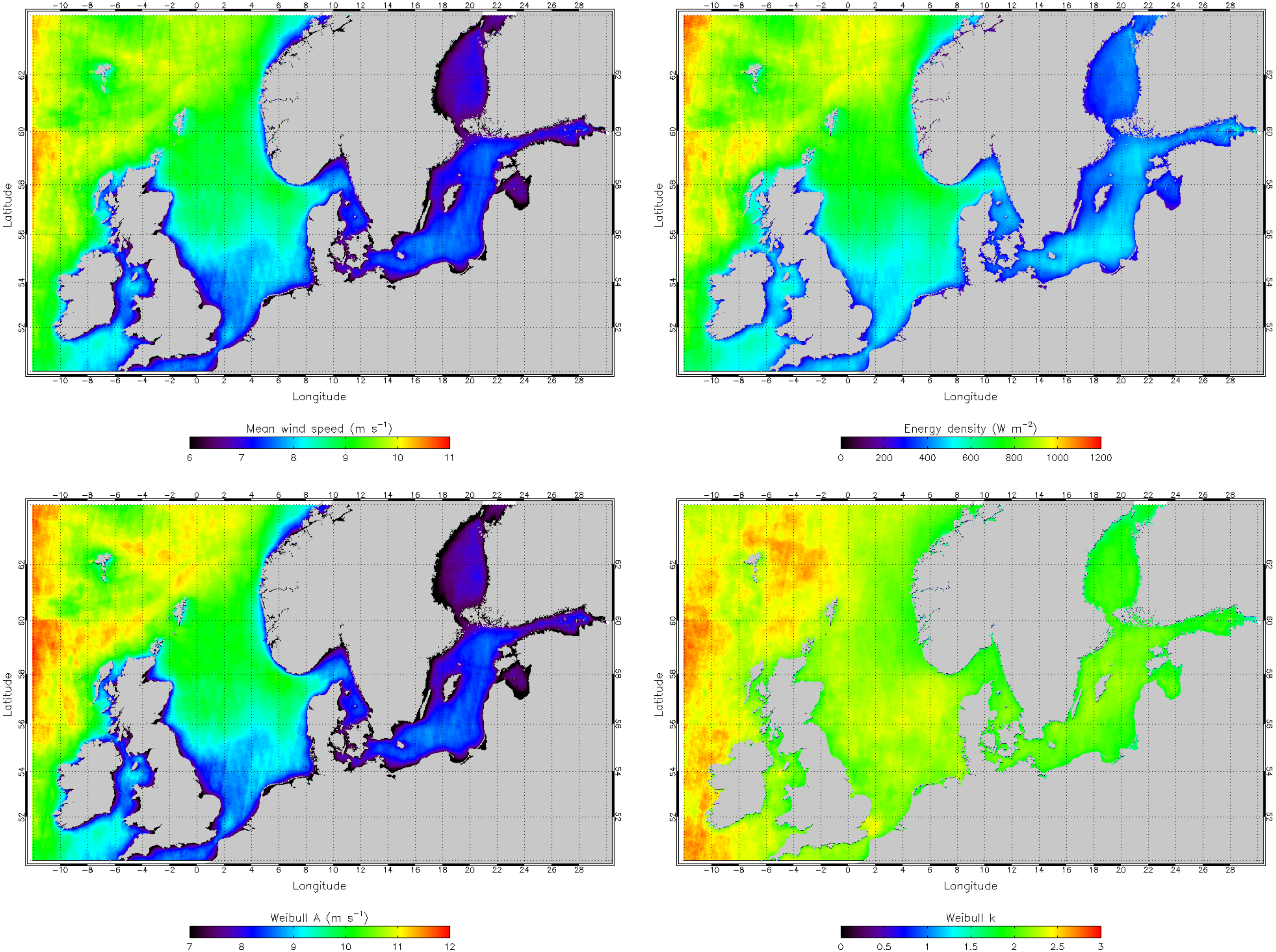
Latitude
Longitude
Mean wind speed (m s^{-1})
6 7 8 9 10 11
Energy density (W m^{-2})
0 200 400 600 800 1000 1200
Weibull A (m s^{-1})
7 8 9 10 11 12
Weibull k
0 0.5 1 1.5 2 2.5 3

Baltic Sea existing and planned offshore wind farms

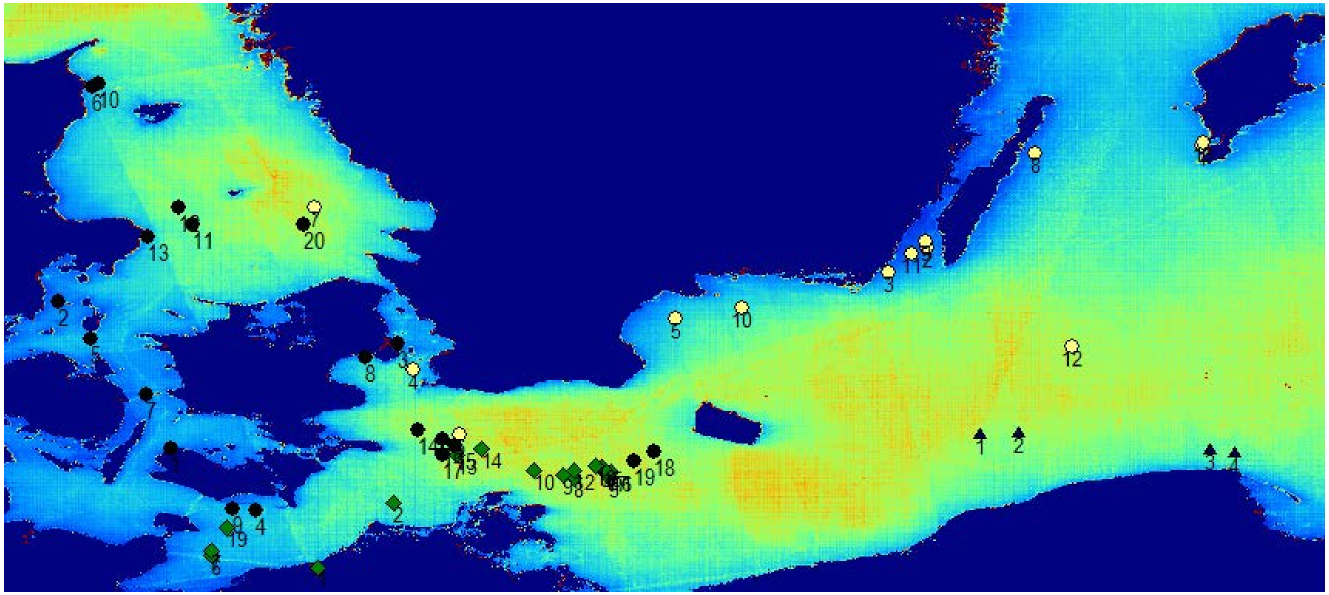

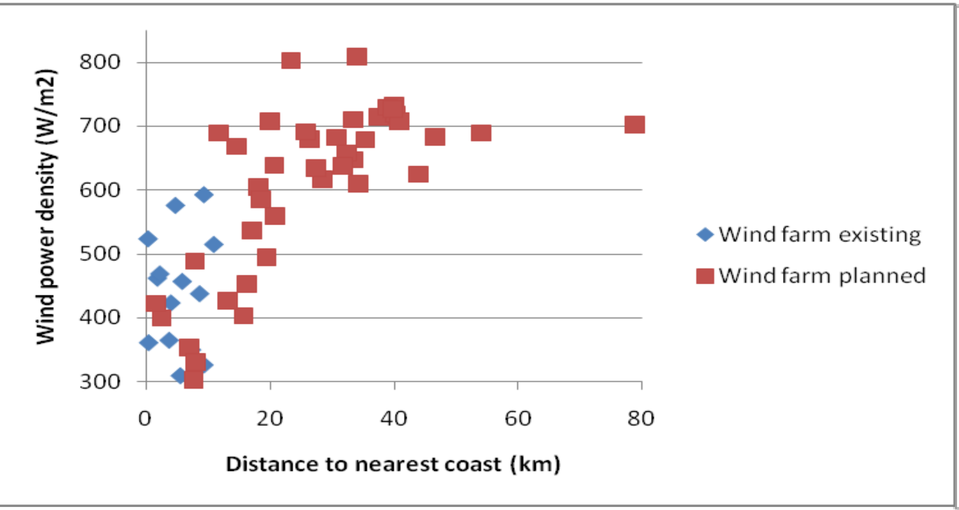

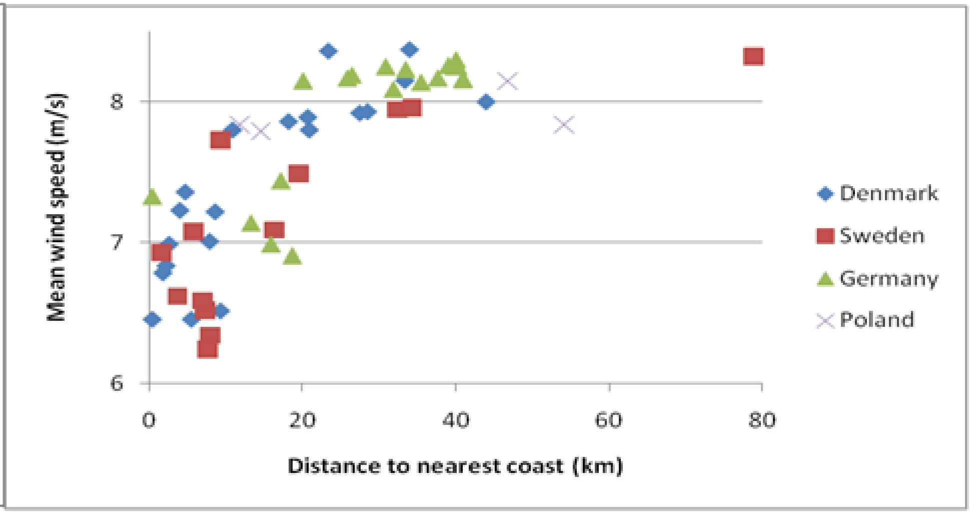

Hasager, C.B., Badger, M., Peña, A, Larsén, X.G. 2011 SAR-based wind resource statistics in the Baltic Sea, *Remote Sensing.* 2011, 3(1), 117-144 ; doi:10.3390/rs3010117

Model validation

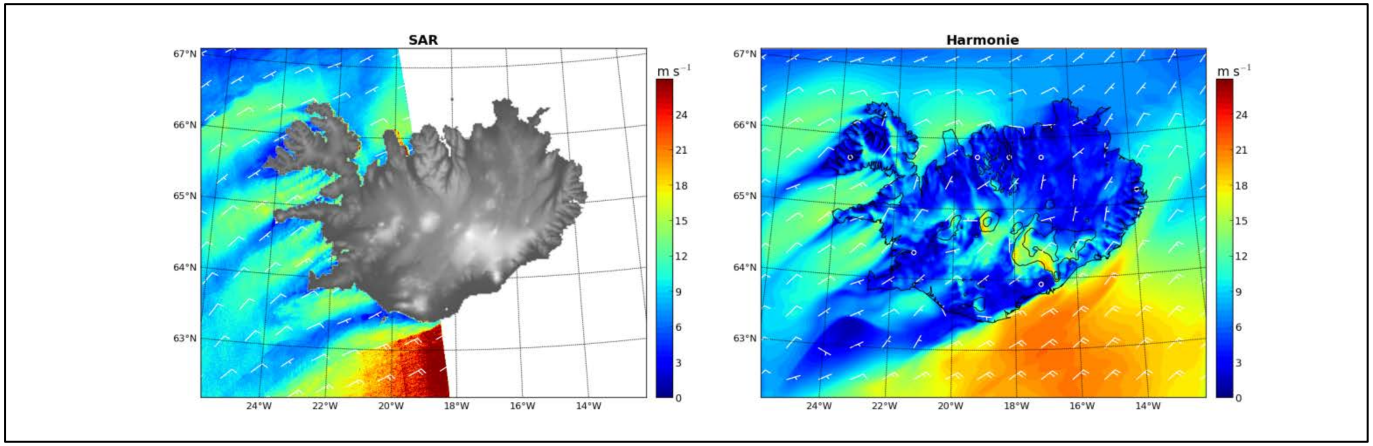

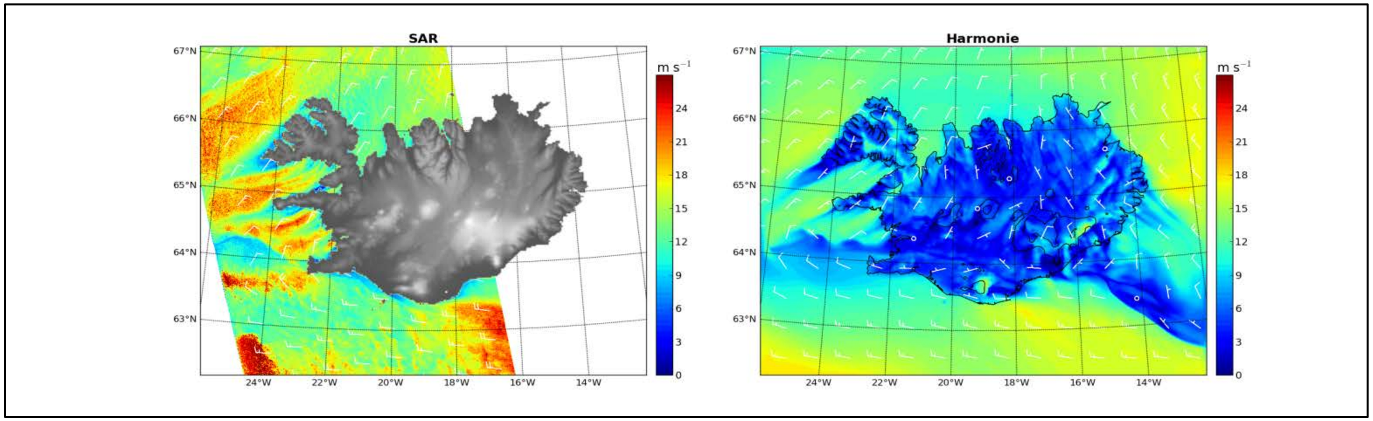

Hasager, C.B., Badger, M. Nawri, N., Furevik, B.R., Petersen, G. N., Björnsson, H., Clausen, N.-E. (2015) Mapping offshore winds around Iceland using satellite Synthetic Aperture Radar and mesoscale model simulations. *IEEE Journal of Selected Topics in Applied Earth Observations and Remote Sensing*, [10.1109/JSTARS.2015.2443981](https://doi.org/10.1109/JSTARS.2015.2443981)

Wind atlas output and verification

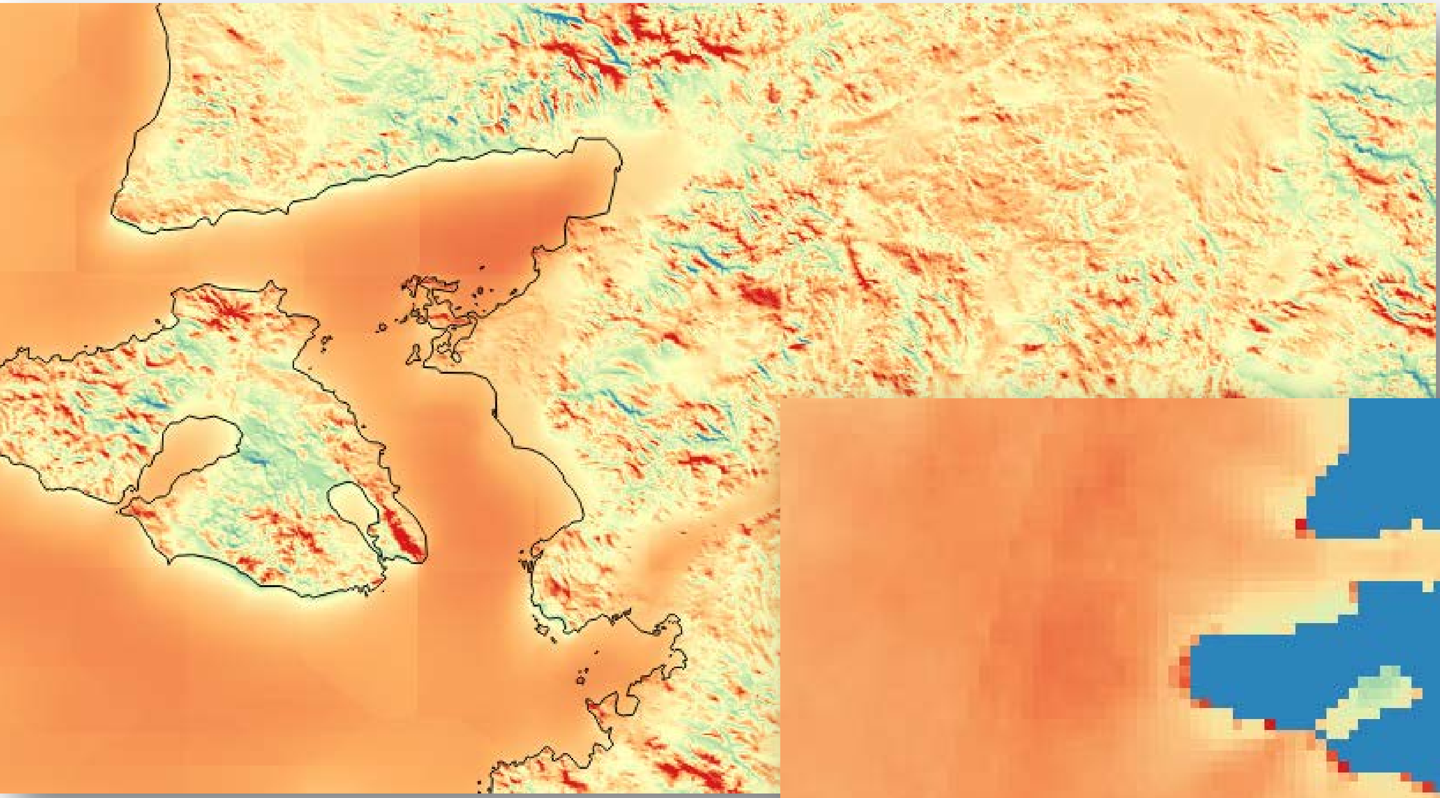

Mean wind speed from the IRENA Global Wind Atlas

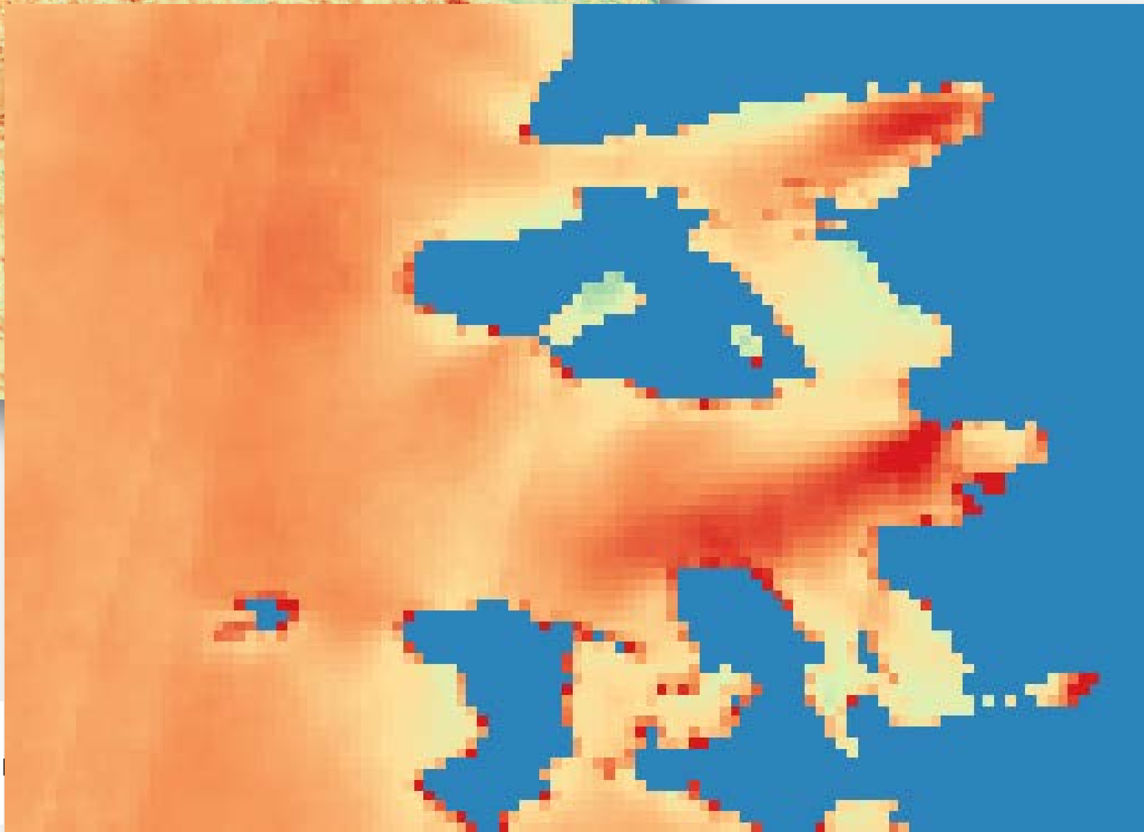

Mean wind speed from Envisat ASAR

Wind farm wakes

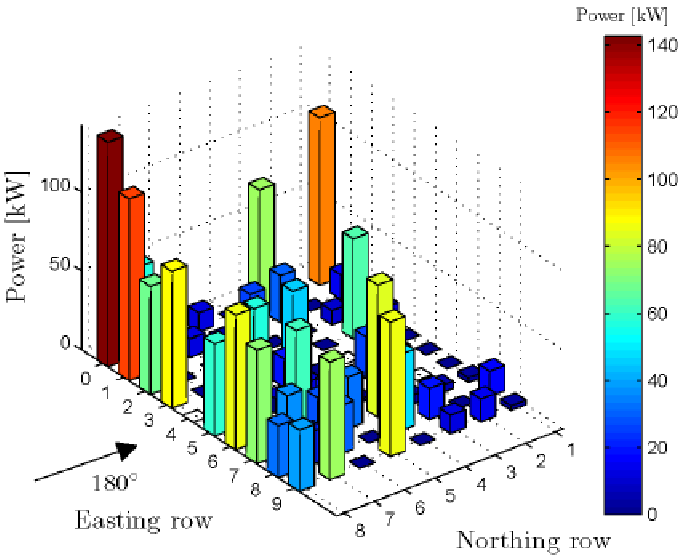

Hasager, C.B., Rasmussen, L., Peña, A., Jensen, L.E., Réthoré, P.-E., 2013, Wind farm wake: The Horns Rev photo case, *Energies*, *6*(2), 696-716; doi:10.3390/en6020696

Wind farm wake from SAR

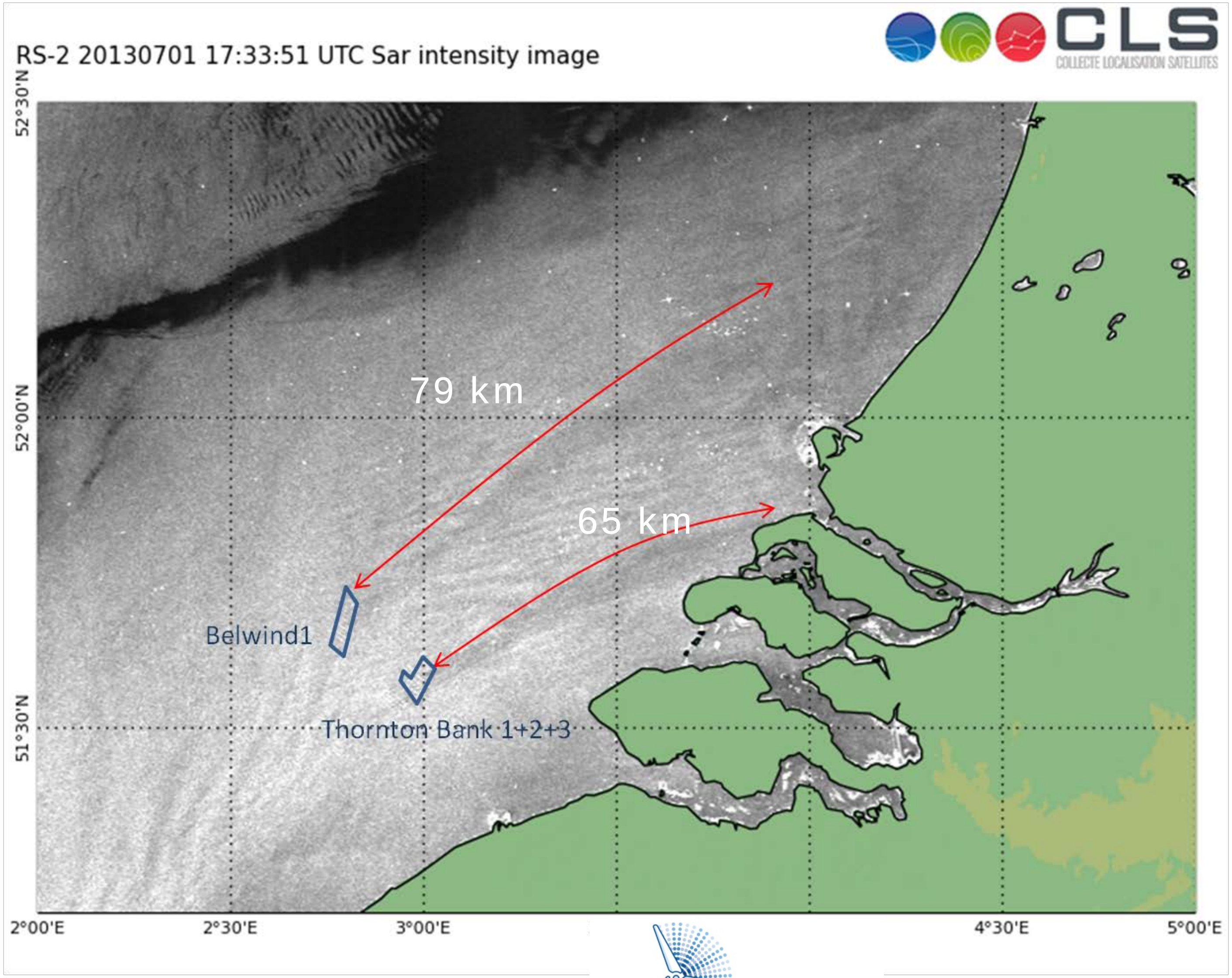

Radarsat-2, 2013/07/01 17:33

Image courtesy CLS, France

Offshore wind farm wake

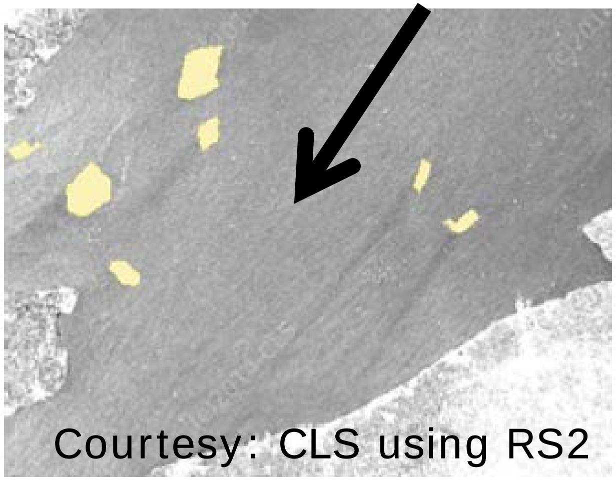

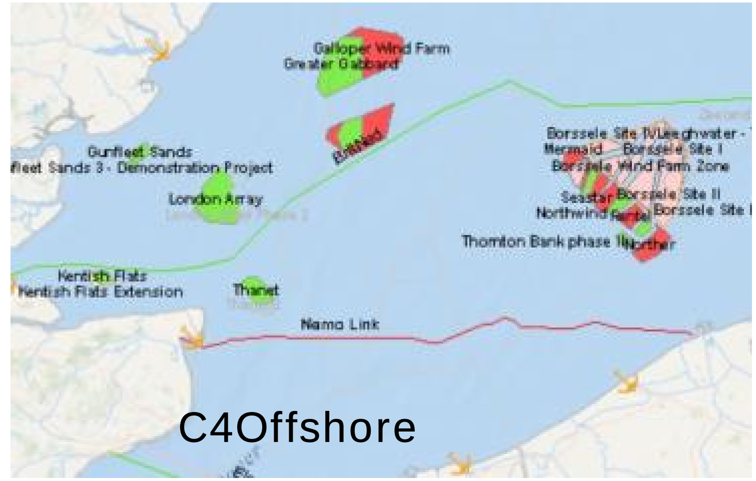

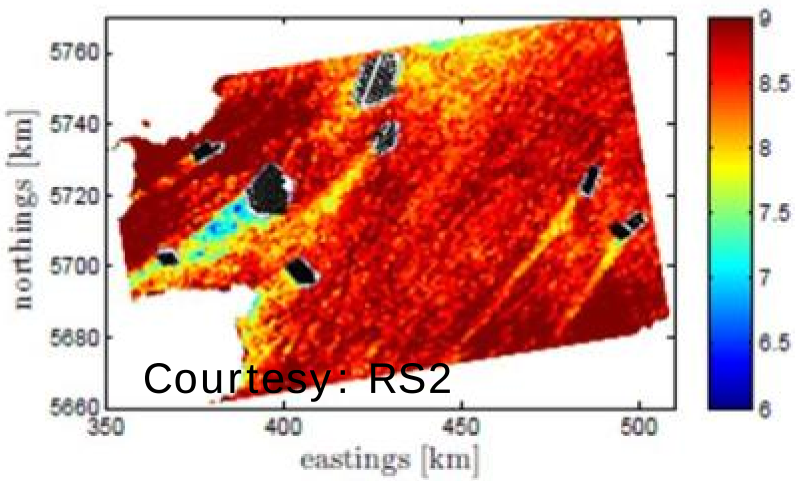

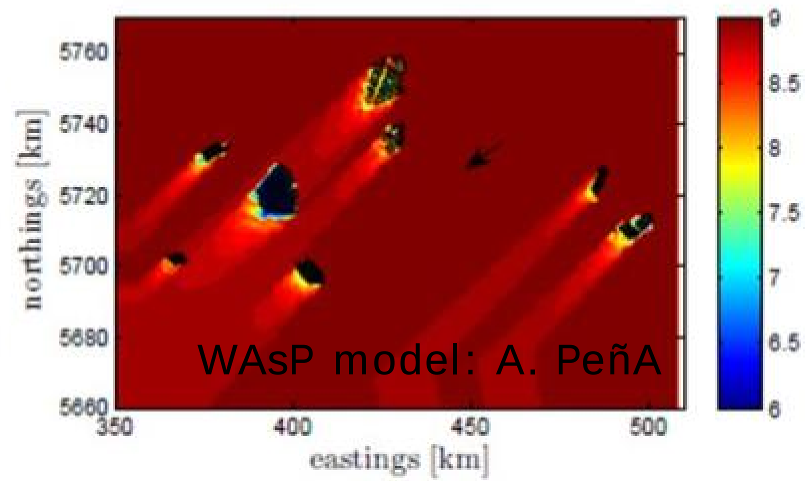

Hasager, C.B., Vincent, P., Badger, J., Badger, M. Di Bella, A., Peña, A. Husson, R., Volker, P. (2015) Using satellite SAR to characterize the wind flow around offshore wind farms. *Energies, 8*(6), 5413-5439; doi:[10.3390/en8065413](https://doi.org/10.3390/en8065413)

Motivation for lifting winds to hub-height

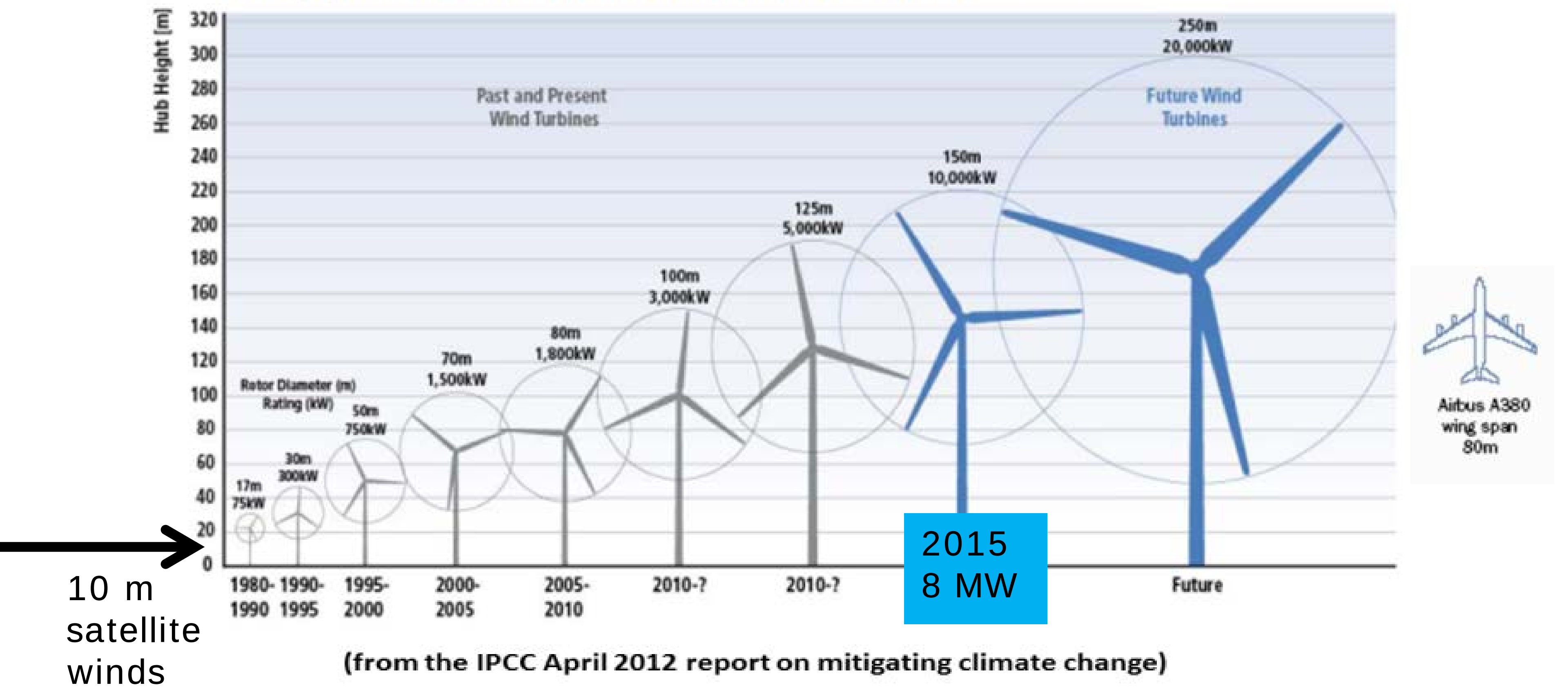

(from the IPCC April 2012 report on mitigating climate change)

Wind profile equation

The equation to estimate the mean wind speed at height above the ground is:

$$u_z = \frac{u_*}{\kappa}\left[\ln\left(\frac{z-d}{z_0}\right) + \psi(z, z_0, L)\right]$$

.

Long-term histograms of stability

Mast observations

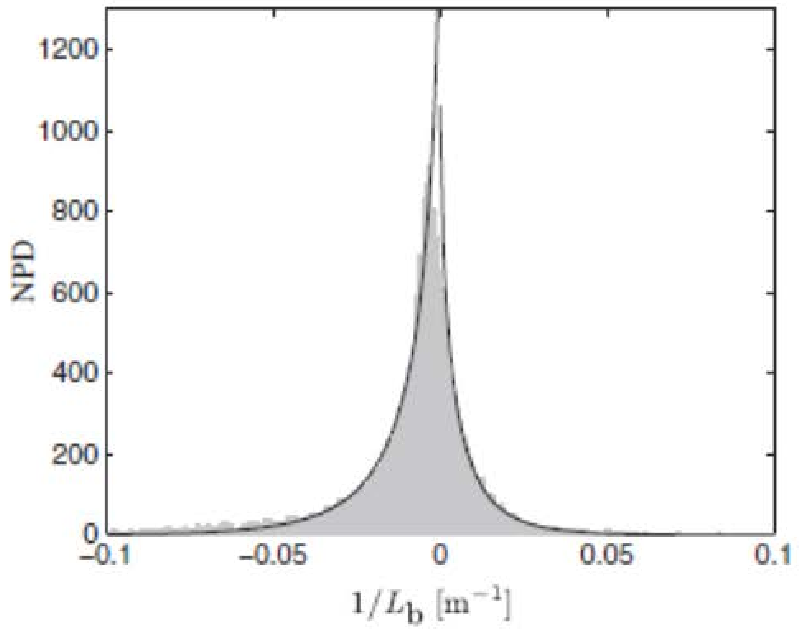

WRF model data

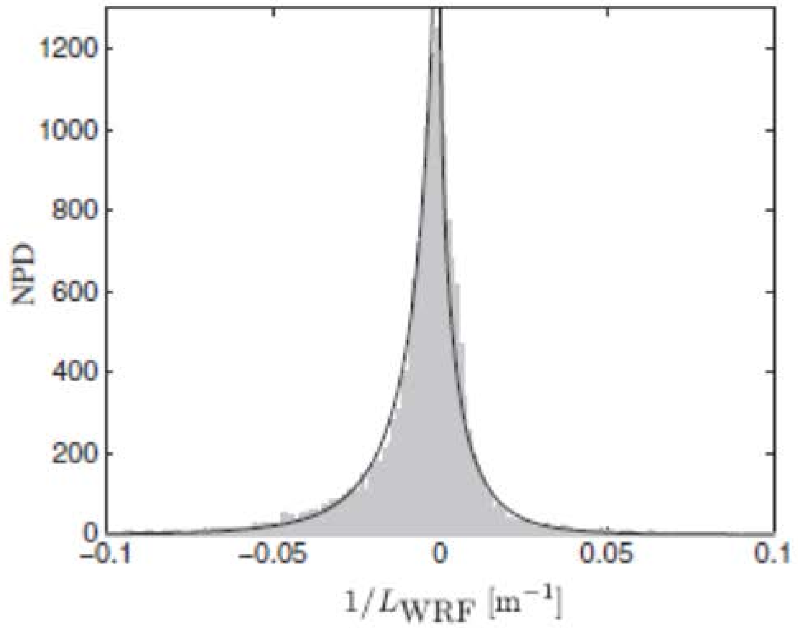

Theoretical lines are based on: Kelly, M. and Gryning, S.-E. (2010), Long-term mean wind profiles based on similarity theory, *Boundary-Layer Meteorology*, 136, 377-390.

Long-term stability correction from WRF

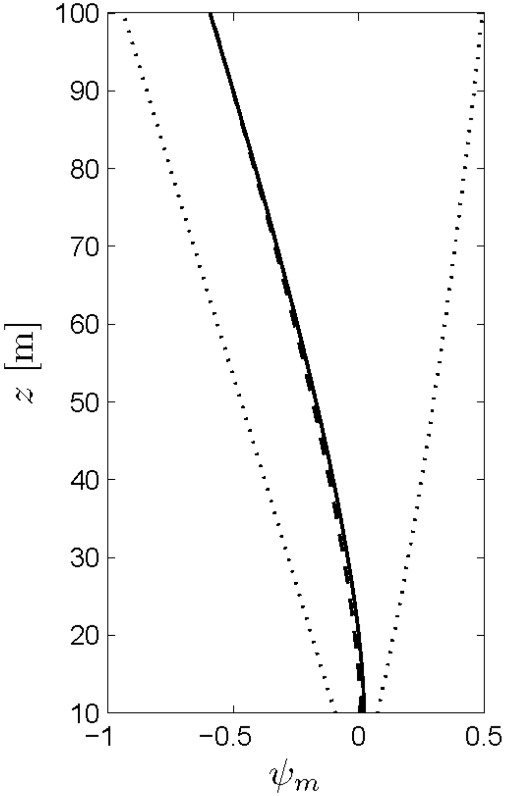

Horns Rev M2 mast

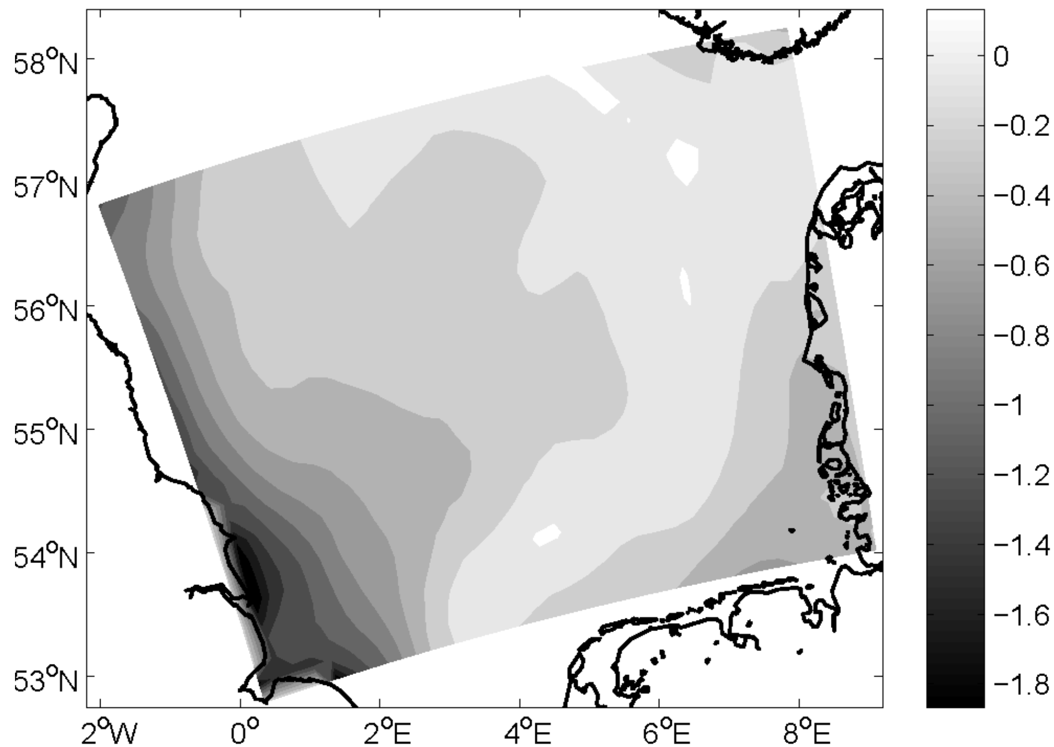

The North Sea

Peña, A. & Hahmann, A.N. 2012, Atmospheric stability and turbulence fluxes at Horns Rev – an intercomparison of sonic, bulk and WRF model data, *Wind Energy*, *15*, 717-731, DOI: 10.1002/we.500.

Friction velocity from the satellite *ENW*:

$$u_{10\,SAR} = \frac{u_{*\,SAR}}{\kappa}\left[\ln\frac{10}{z_0}\right] \qquad \text{where} \qquad z_0 = \alpha_c \frac{u_{*SAR}^2}{g}$$

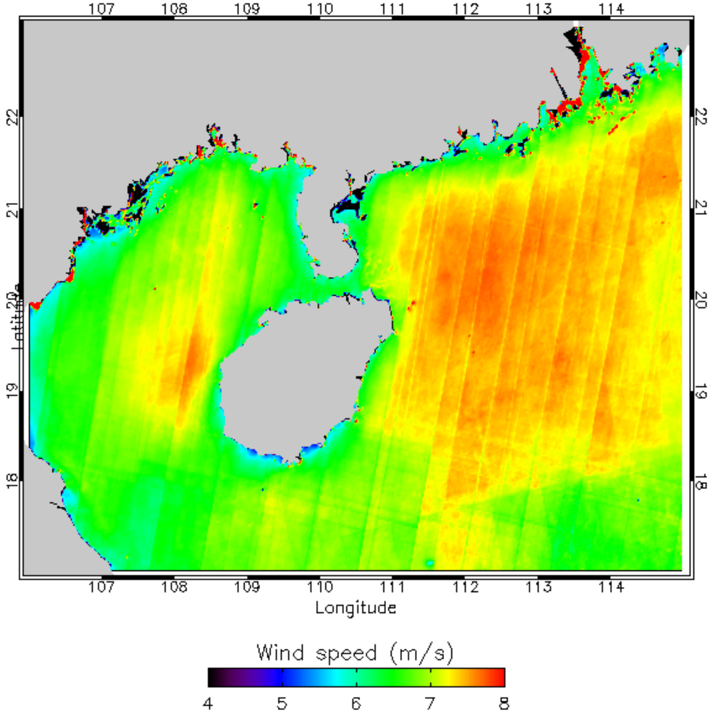

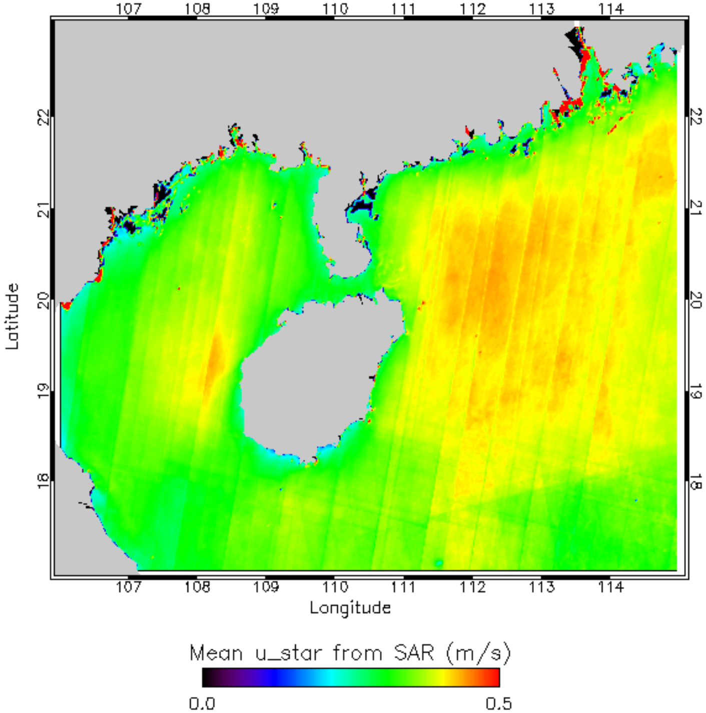

Frequency distribution of 1/L

$$L_{WRF} = -\frac{UST^3\,T2}{g\,\kappa\,HFX}$$

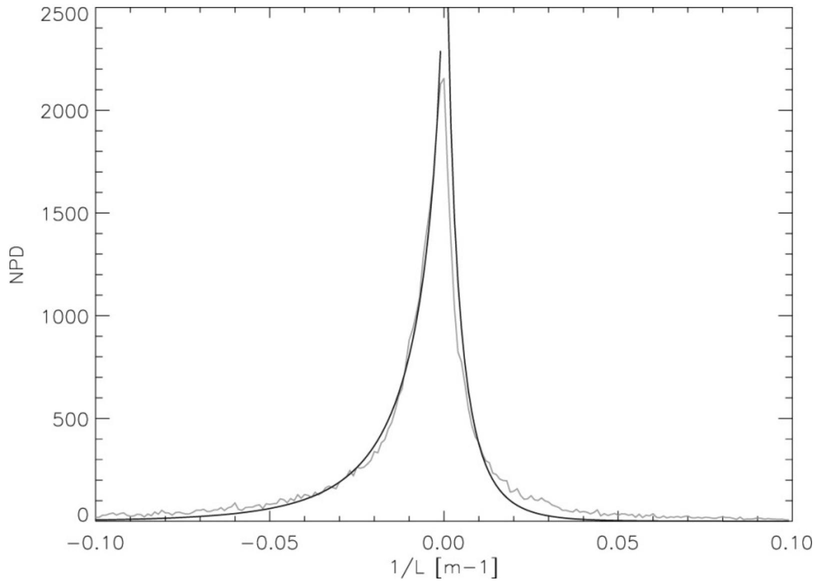

Baltic Sea: 6 years of WRF

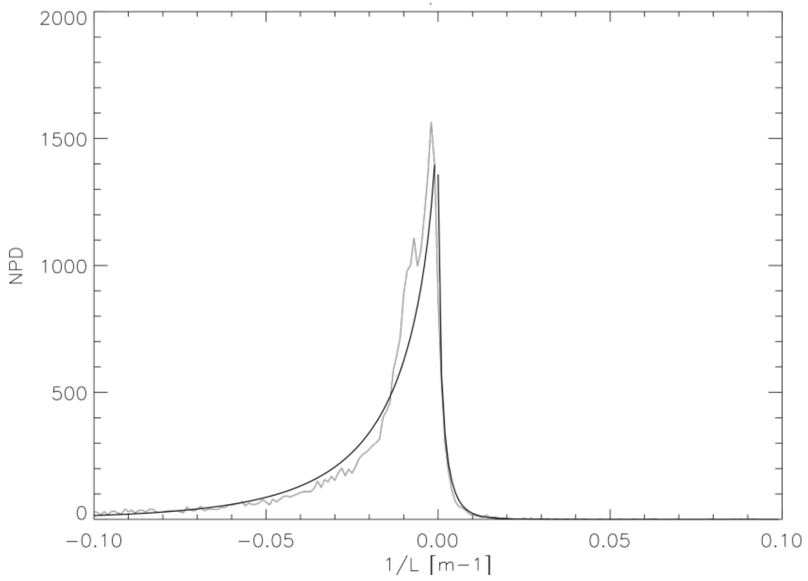

South China Sea: 3 years of WRF

Long-term stability correction profiles

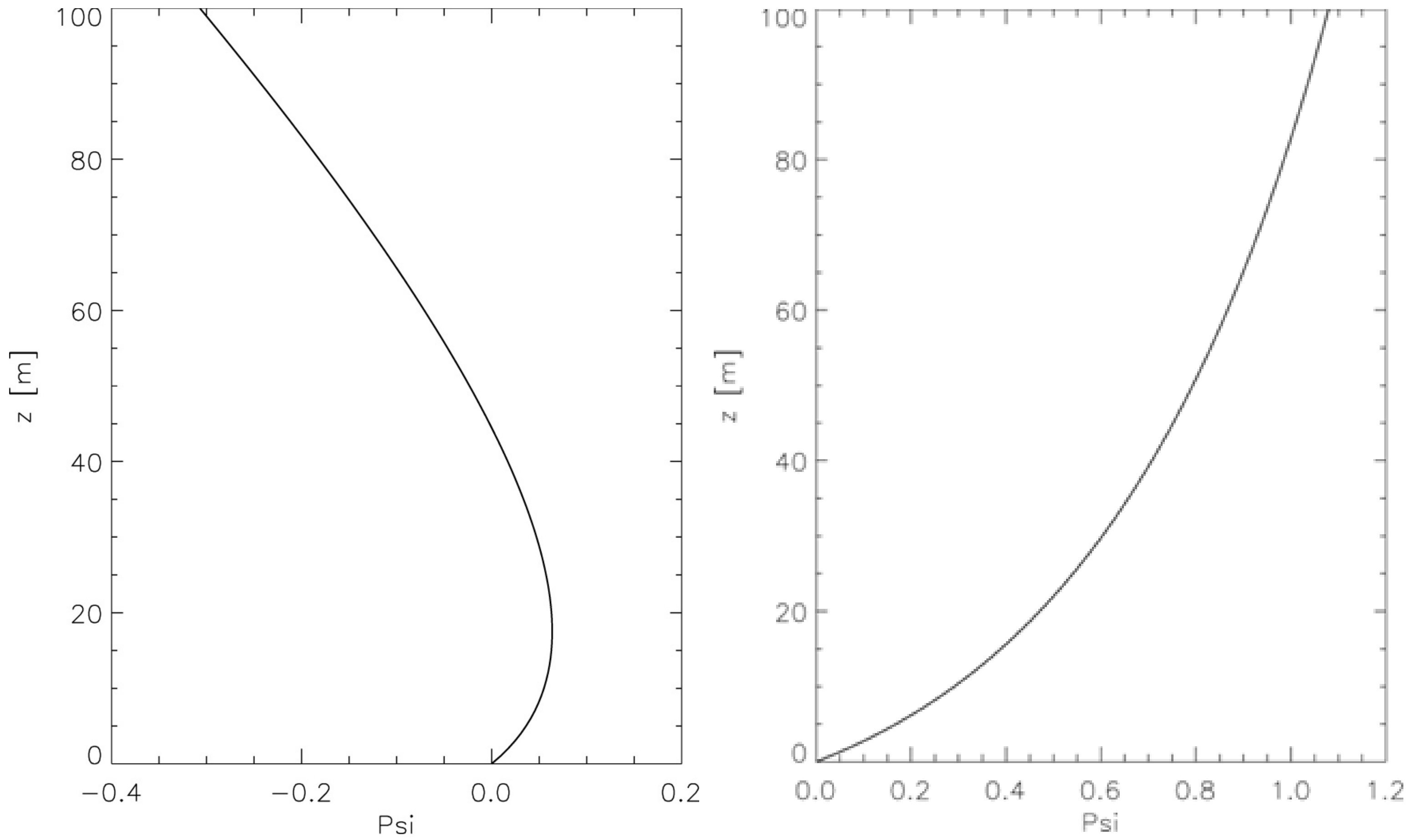

Baltic Sea *South China Sea*

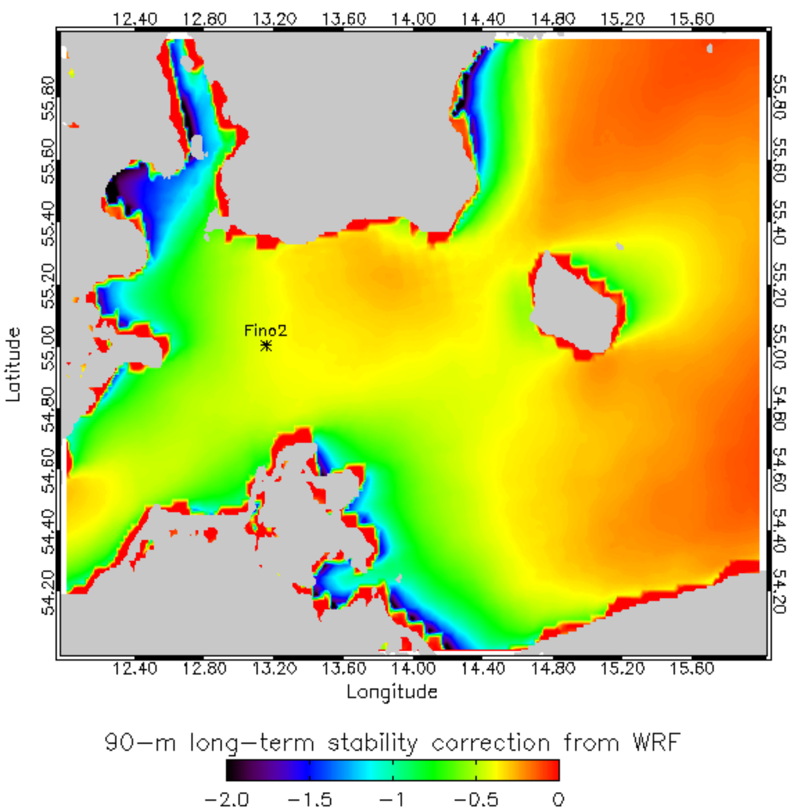

Baltic Sea

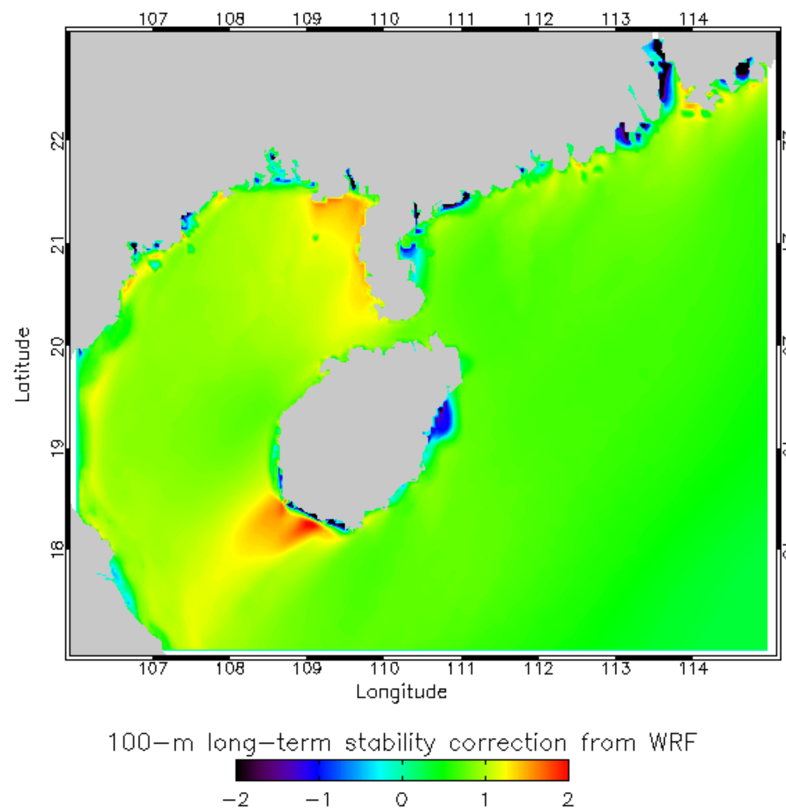

South China Sea

Mean wind speed at 100 m

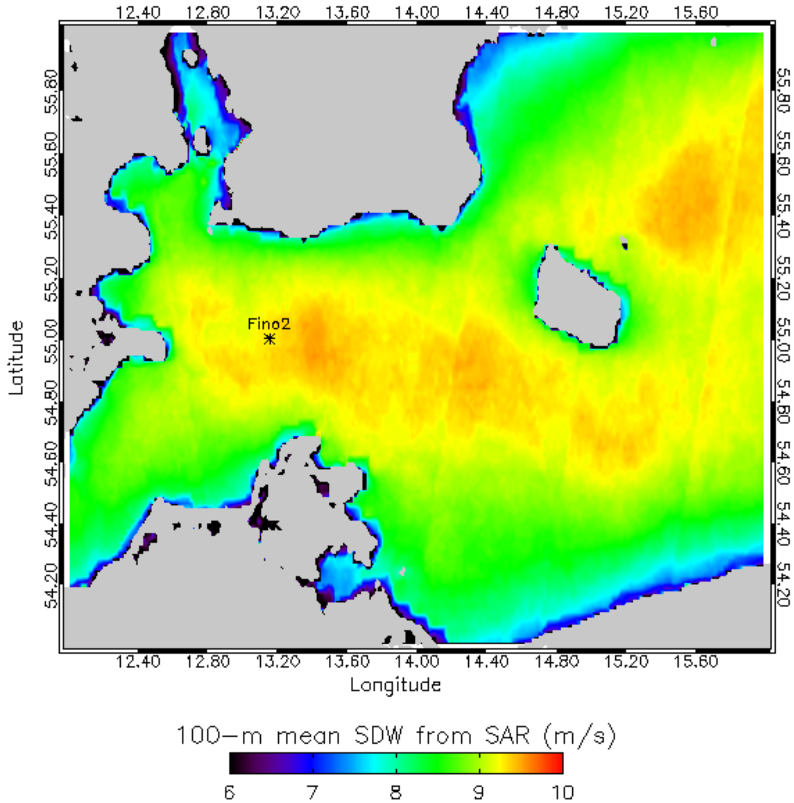

Baltic Sea

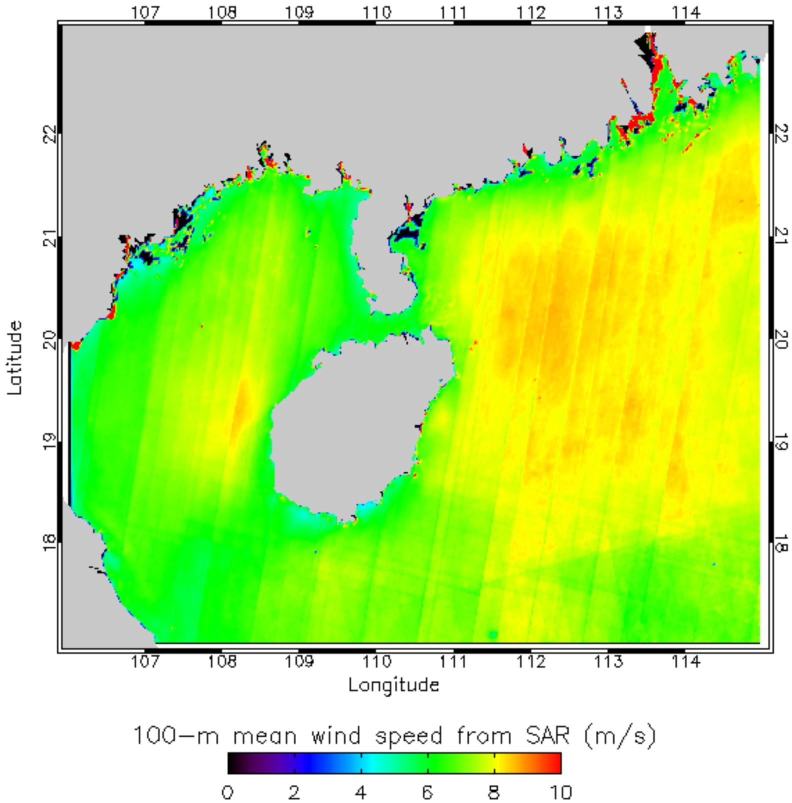

South China Sea

Badger, M., Peña. A., Hahmann, A.N., Mouche, A., Hasager, C.B. (2015) Extrapolating satellite winds to turbine operating heights. *JAMC* (in review)

Summary of SAR advantages and limitations

<u>Advantages:</u>

- A high spatial resolution (sufficient to reveal meso-scale wind phenomena)
- Coastal seas are covered (still the most important for offshore wind energy applications)

<u>Limitations:</u>

- Wind retrievals are valid for the height 10 m
- A limited number of samples exists for statistical analyses

Acknowledgements

Satellite data:

The European Space Agency (ESA)

EUMETSAT Ocean and Sea Ice Satellite Application Facility

Remote Sensing Systems (RSS)

SAR wind field retrieval:

The Johns Hopkins University, Applied Physics Laboratory (JHU/APL)

Collecte Localisation Satellites (CLS)

Mast observations:

All mast data accessed through the NORSEWInD project. Horns Rev: DONG energy and Vattenfall, Fino-1 and Fino-2: Deutsches Windenergie Institut, Egmond an Zee: NoordZeewind, Greater Gabbard: SSE Renewables.

Funding:

EU-NORSEWInD, EU South Baltic OFFER, Nordic Icewind, Sino-Danish ORES, EU EERA-DTOC, EUDP Global Wind Atlas, ESA ResGrow, ERANET plus NEWA